2014

Group Velocity Of Acoustic Waves In Plates Of Electronic Materials

Saminda Adikaram
University of Mississippi

GROUP VELOCITY OF ACOUSTIC WAVES IN PLATES OF ELECTRONIC MATERIALS

A Thesis
presented in partial fulfillment of requirements
for the degree of Master of Science
in the Department of Physics and Astronomy
The University of Mississippi

by

SAMINDA ADIKARAM

May 2014

ABSTRACT

In this study the propagation and dispersion characteristics of plate acoustic waves (PAW) in electronic materials are investigated experimentally. Plate acoustic waves are elastic waves that travel along a plate with thickness comparable to the wavelength of the waves. Lamb waves, a type of plate acoustic wave, have particle motion in the direction of propagation and normal to the plate. Unlike an infinite medium, plates support two sets of Lamb wave modes (symmetric and anti-symmetric) with unique velocities which depend on the relationship between the wavelength and the thickness of the plate. Out of this, two zero order modes (s_o and a_o) in several electronic material plates are studied here. This kind of study has practical applications particularly in non-destructive testing.

Lamb waves are propagated through plates of glass, brass, aluminium and lithium niobate. The delay of propagation of Lamb waves through the plates is measured and the group velocities of the s_o and a_o modes are then computed and plotted against the frequency and the thickness of the plate. These results compare well with the theoretical results obtained from published work. Group velocities of PAW in all of them are found to be similarly dispersive. The s_o mode has a low dispersion when the product of frequency and thickness is lower than approximately 1MHz-mm whereas the a_o mode is less dispersive when the same product is higher than about 1MHz-mm, a characteristic which is usually exploited in industry. Thus it can be concluded that the experimental work matches well with the theory and the analysis can be useful in industrial applications such as testing the uniformity of materials and defect detection.

DEDICATION

This thesis is dedicated to everyone who guided or supported me on the way to achieving this goal, especially to my parents who were always there for me with encouragement.

LIST OF ABBREVIATIONS AND SYMBOLS

$\vec{r}$ – Position vector

$\vec{u}$ – Displacement vector

dl – Displacement of two points before deformation

dl′ – Displacement of two points after deformation

S_{ik} – Strain tensor

dV – Micro-volume before deformation

dV′ – Micro-volume after deformation

$S^{(1)}$, $S^{(2)}$, $S^{(3)}$ – Diagonal components of the strain tensor

dF_i – Force element

p – Pressure

δ_{ik} – Kronecker delta

dA – Surface element

T_{ik} – Stress tensor

W – Work done

V – Volume

U – Internal energy

T – Temperature

S – Entropy

F – Helmholtz free energy

F_0 – Helmholtz free energy at 0 K

λ', μ' – Lamé coefficients

μ - Modulus of rigidity

K – Modulus of compression

χ – Compressibility

c_{ijkl} – Elastic stiffness tensor

Y – Young's modulus

σ – Poisson's ratio

p_i – Pressure of the incident wave

p_r – Pressure of the reflected wave

p_t – Pressure of the transmitted wave

A – Amplitude

ω – Angular frequency

t – Time

k_i – Wave vector in a particular medium

R_p – Pressure reflection coefficient

T_p – Pressure transmission coefficient

Z – Characteristic acoustic impedance

I_i – Intensity of the incident wave

I_r – Intensity of the reflected wave

I_t – Intensity of the transmitted wave

SWR – Standing wave ratio

$P_{antinode}$ – Pressure of antinode

P_{node} – Pressure of node

$\vec{I}$ – Poynting's vector

v^* – Particle velocity

θ_I, θ_r, θ_t – Angles of incidence, reflection and transmission

c_{44} – Term in the 4th column and 4th row of the elastic stiffness tensor

ϕ – Scalar potential

ψ – Vector potential

k_L, k_S – Bulk wave numbers

γ – Propagation constant / wave vector

ρ – Density

γ_L, γ_S – Variations of displacements with z

η, ξ - Potential functions depending on Poisson's ratio

V_D – Dilatational wave velocity

V_S – Shear wave velocity

V_R – Rayleigh velocity

V_{Lm} – Lamé velocity

λ = Wavelength

b = Half plate thickness

k_{tl}, k_{ts} – Transverse wave numbers

V_L – Longitudinal wave velocity

V_P – Phase wave velocity

E – Electric field

D – Electric displacement

H – Magnetic field

θ - Temperature

U_m = Mutual energy between electrical and acoustic energy

U_e = Elastic energy

U_d = Dielectric energy

F_i – Acoustic force

V_i – Terminal velocity

ω_0 – Synchronous frequency

v – Acoustic velocity

l – Periodic length of the system

K – Effective electromechanical coupling constant

f – Filling factor

u – Particle displacement

V_e = Energy propagation velocity

V_G – Group velocity

ε – Permittivity

P – Polarization

e – Piezoelectric stress constant

h_{ij} – Transmitting constant

g – Receiver constant

K^2 – Piezoelectric coupling constant

k_T^2 – Effective coupling constant in plate vibrator

m - Minimum measurement of an instrument

x – Value of the measurement

k – Wave number

h – Piezo constant

ACKNOWLEDGEMENTS

First and foremost I would like to thank Dr. Igor Ostrovskii, my research advisor, for giving me the opportunity to work under his guidance on this research topic and for the support, encouragement and direction provided towards the completion of this thesis. His guidance and help in understanding related subject matter, demonstrative guidance in handling laboratory equipment and conducting experiments, advice in technical writing along with thesis preparation and the knowledge passed on is greatly appreciated. My special thanks to the committee members of my defence, Dr. Lucien Cremaldi, Dr. Igor Ostrovskii and Dr. Tibor Torma for taking their valuable time to evaluate my work. I want to express my gratitude to Dr. Tibor Torma for supporting me throughout with teaching assistantships and the advice given. I would also like to thank Dr. Luca Bombelli for all the support as the graduate coordinator during my time of study. Additionally The Department of Physics and Astronomy and The Graduate School, University of Mississippi must be thanked for making this a reality with support in the form of teaching assistantships, summer research assistantships and scholarships. Finally I'm grateful to my friends and family for their moral support throughout this journey and to anyone, even if their names are not mentioned here, who had a hand in this in some way.

TABLE OF CONTENTS

LIST OF TABLES

LIST OF FIGURES

CHAPTER 1

BASICS OF PHYSICAL ACOUSTICS IN SOLIDS

1.1 Introduction

1.1.1 Tensors

Scalars are physical quantities that can be represented by numerical values whereas vectors are associated with a direction while also having a magnitude. Tensors are geometric objects that describe linear relations between scalars, vectors and other tensors. They are essential in describing the correspondence between two geometrical vectors in anisotropic media and even in isotropic media when coming across quantities with three components. A scalar is a tensor of rank zero while a vector is a tensor of rank one. Although a tensor is represented in matrix form it is actually a real physical quantity. A tensor is also defined by the way it transforms under coordinate transformation.

1.1.2 Strain Tensor

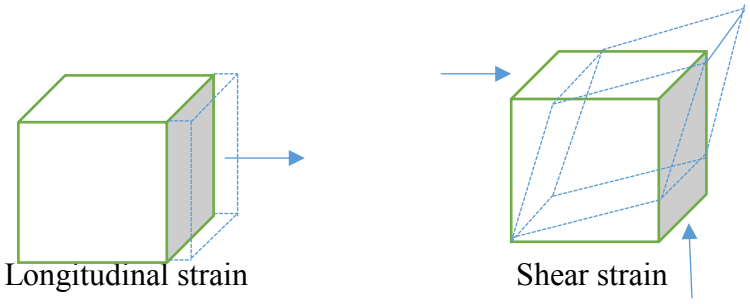

Fig. 1.1: Deformation when longitudinal or shear strain is applied to a cube

Strain tensor is used to describe the deformation caused by forces applied in solids. If the displacement is from position vectors $\vec{r}$ to $\overrightarrow{r'}$, the displacement vector is $\vec{u} = (\overrightarrow{r_i'} - \vec{r})$ or in tensor notation $u_i = (x_i' - x_i)$. If the displacement of two points nearby due to deformation is dl before and dl′ after [1],

$$dl'^2 = dl^2 + 2\,\frac{\partial u_i}{\partial x_k}\,dx_i\,dx_k + \frac{\partial u_i}{\partial x_k}\,\frac{\partial u_i}{\partial x_l}\,dx_k\,dx_l \tag{1.1}$$

This can be written as,

$$dl'^2 = dl^2 + 2S_{ik}dx_i dx_k \tag{1.2}$$

Where,

$$S_{ik} = \frac{1}{2}\left(\frac{\partial u_i}{\partial x_k} + \frac{\partial u_k}{\partial x_i} + \frac{\partial u_l}{\partial x_i}\,\frac{\partial u_l}{\partial x_k}\right) \quad \text{is the strain tensor.} \tag{1.3}$$

If strains are small this becomes,

$$S_{ik} = \frac{1}{2}\left(\frac{\partial u_i}{\partial x_k} + \frac{\partial u_k}{\partial x_i}\right) \tag{1.4}$$

Diagonal terms in the stress tensor correspond to compression or expansion along the three axes. Non-diagonal terms correspond to the deformation of the plane perpendicular to the z axis. The change in angle of the two sides of a rectangle is proportional to the Shear strain S_{xy}. Any symmetric tensor can be diagonalised at a point by the choice of appropriate axes, then the non-diagonal terms become zero. The trace of a symmetric tensor is invariant under the change of coordinates.

$$\sum S_{ii} = S_{11} + S_{22} + S_{33} \tag{1.5}$$

If the micro-volumes before and after the deformation are dV and dV' respectively,

$$dV' = dV\,(1 + S^{(1)})(1 + S^{(2)})(1 + S^{(3)}) \tag{1.6}$$

where $S^{(1)}$, $S^{(2)}$ and $S^{(3)}$ are diagonal components.

$$dV' \approx dV\,(1 + S^{(1)} + S^{(2)} + S^{(3)}) \tag{1.7}$$

This becomes,

$$dV' = dV\,(1 + S_{ii}) \tag{1.8}$$

As seen, S_{ii} refers to the relative change in the volume under deformation. This is the same as the dilatation, which is the change in volume per unit volume.

1.1.3 Stress Tensor

A solid body in static equilibrium (figure 1.2) is considered. External forces acting on this object are assumed to cause a deformation rather than a translation or rotation. This deformation can be described by the strain tensor. The stress created by this is generally not uniformly distributed. Consequently the stress applied at a point is different from the stress over the whole area.

In three dimensions, this applied stress has a vector in the direction of the surface normal and the direction of the force. Thus the stress at a specific point in the object is defined by a second rank tensor which is called the stress tensor, in which the first index gives the direction of the force and the second gives the direction of the normal to the surface which it acts upon.

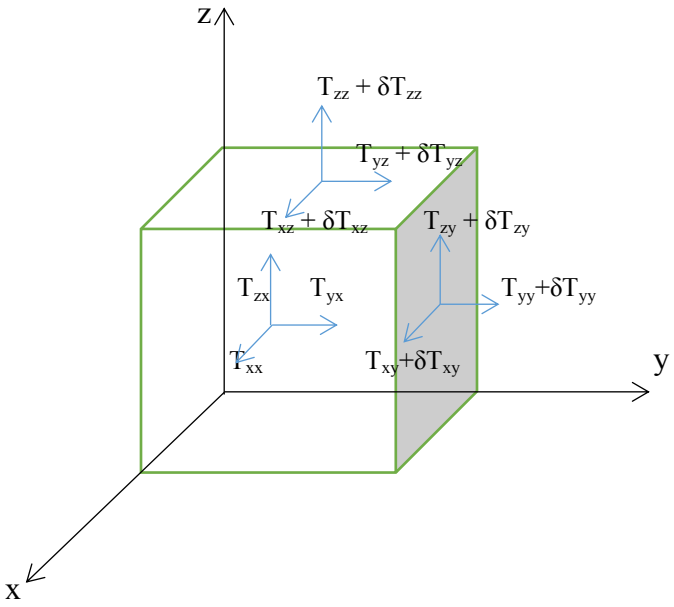

Fig. 1.2: Components of the stress tensor acting on a cube

The force applied will generally be at an arbitrary direction. The components of this force can be separated in to two major classes. The normal component to the face which gives rise to compressive and tensile stresses and the tangential components which gives rise to shear stresses.

Due to the static equilibrium of the object, tensile stresses along any axis must balance to avoid acceleration and so does the shear stresses in order to avoid rotation. These lead to three independent diagonal and three off-diagonal stresses respectively.

For comparison, in the case of a liquid where pressure is uniform in all directions, the force on a surface element dA is,

$$dF_i = -p\,\delta_{ik}\,dA_k = T_{ik}\,dA_k \tag{1.9}$$

where,

p – pressure

δ_{ik} – Kronecker delta

$T_{ik} = -p\ \delta_{ik}$ = stress tensor

$$T_{ik} = \begin{pmatrix} -p & 0 & 0 \\ 0 & -p & 0 \\ 0 & 0 & -p \end{pmatrix}$$

The non-diagonal elements, which correspond to shear stresses, are zero because liquids cannot support them.

1.1.4 Thermodynamics of deformation

Slow and small deformations are assumed so that the processes are elastic and also reversible. For hydrostatic compression, the work done on the system,

$$dW = -p\ dV = T_{ik}\, dS_{ik} \tag{1.10}$$

Then the thermodynamic identity becomes,

$$dU = T\, dS + T_{ik}\, dS_{ik} \tag{1.11}$$

The Helmholtz free energy can be expressed as,

$$F = U - TS \tag{1.12}$$

$$dF = -S\, dT + T_{ik} dS_{ik} \tag{1.13}$$

So,

$$T_{ik} = \left(\frac{\partial F}{\partial S_{ik}}\right)_T \tag{1.14}$$

Piezoelectricity is the accumulation of electric charge in response to an applied mechanical stress. Piezoelectric constitutive relations are written as one dependent variable

depending on two independent variables, of which one is an electrical quantity and the other mechanical. They are broken into four pairs of equations with each pair containing a different combination of the two variables as follows,

a) T and E are independent

$$S_{ij} = s^E_{ijkl} T_{kl} + d_{ij} E_j \quad (1.15)$$

$$D_i = d_{ij} T_{kl} + \varepsilon^T_{ij} E_j$$

b) T and D are independent

$$S_{ij} = s^D_{ijkl} T_{kl} + g_{ij} D_i \quad (1.16)$$

$$E_j = -g_{ij} T_{kl} + \beta^T D_i$$

c) S and E are independent

$$T_{kl} = c^E_{ij} S_{ij} - e_{ijk} E_j \quad (1.17)$$

$$D_i = e_{ijk} S_{ij} + \varepsilon^S_{ij} E_j$$

d) S and D are independent

$$T_{kl} = c^D_{ij} S_{ij} - h_{ij} D_i \quad (1.18)$$

$$E_j = -h_{ij} S_{ij} + \beta^S D_i$$

where,

D – electric displacement

E – electric field

e – piezoelectric stress constant

β – dielectric impermeability

$$s_{ijkl} = \frac{\partial S}{\partial T}$$

$$d_{ij} = \left(\frac{\partial S}{\partial E}\right)_T = \left(\frac{\partial D}{\partial T}\right)_E$$

$$\varepsilon_{ij} = \frac{\partial D}{\partial E} = \text{permittivity}$$

$$h_{ij} = \left(-\frac{\partial T}{\partial D}\right)_S = \left(-\frac{\partial E}{\partial S}\right)_D = \text{transmitting constant}$$

$$g_{ij} = \left(-\frac{\partial E}{\partial T}\right)_D = \left(\frac{\partial S}{\partial D}\right)_T = \text{receiver constant}$$

The receiver constant g, determines the potential drop across a transducer for an applied stress. It can be expressed as,

$$g = \frac{d}{\varepsilon^T} \tag{1.19}$$

where,

$\varepsilon^T = \left(\frac{\partial D}{\partial E}\right)_T$ is a proportionality constant.

Transmitting constant h, gives the electric field needed to produce a certain strain. It can be expressed as,

$$h = \frac{e}{\varepsilon^S} \tag{1.20}$$

1.1.5 Hooke's law

Hooke's law states that for small elongations of an elastic system, the stress is proportional to the applied strain. For an isotropic solid, Hooke's law can be approached in terms of the Helmholtz free energy (F), which can be expanded at constant temperature as [1],

$$F = F_0 + \frac{1}{2}\lambda' \sum_i u_{ii}^2 + \mu' \sum_{i,k} S_{ik}^2 \quad (1.21)$$

where λ' and μ' are the Lamé coefficients that describes the elastic properties of an isotropic solid.

Since the strain tensor is symmetric and the trace of any tensor is independent of any coordinate system, the most complete coordinate-free decomposition of a symmetric tensor is to represent it as the sum of a constant tensor and a traceless symmetric tensor,

$$S_{ik} = \left(S_{ik} - \frac{1}{3}\,\delta_{ik}\,\sum_{l=1}^{3} S_{ll}\right) + \frac{1}{3}\,\delta_{ik}\sum_{l=1}^{3} S_{ll} \quad (1.22)$$

The first term is pure shear deformation and the second is hydrostatic compression. Now the Helmholtz free energy becomes,

$$F = \mu\left(S_{ik} - \frac{1}{3}\,\delta_{ik}\,S_{ll}\right)^2 + \frac{1}{2}\,K\,S_{ll}{}^2 \quad (1.23)$$

μ - modulus of rigidity

$K = \lambda + 2/3\ \mu$ = modulus of compression

These two moduli determine the velocities of longitudinal and shear modes. At a given temperature, Helmholtz energy is a minimum when a system is in thermal equilibrium. Pure compression and shear deformation give rise to stress components proportional to K and μ respectively.

Compressibility can be expressed as,

$$\chi = \frac{1}{K} = -\frac{1}{V}\left(\frac{\partial V}{\partial p}\right)_T \quad (1.24)$$

Then it can be shown that,

$$F = \frac{1}{2} T_{ik} S_{ik} \tag{1.25}$$

In another approach to the Hooke's law, the stress tensor is Taylor expanded around S_{kl}, which yields,

$$T_{ij} = c_{ijkl} S_{kl} \tag{1.26}$$

Where c_{ijkl} is the elastic stiffness tensor or elastic constant tensor (c_{IJ} is the reduced notation) which is given by,

$$c_{ijkl} = \left(\frac{\partial T_{ij}}{\partial S_{kl}}\right)_{S_{kl}=0} = c_{IJ} \tag{1.27}$$

I, J = 1, 2, 3, 4, 5, 6

Also, for an isotropic solid,

$$c_{ijkl} = \lambda \delta_{ij} \delta_{kl} + \mu(\delta_{ik} \delta_{jl} + \delta_{il} \delta_{jk}) \tag{1.28}$$

c_{ijkl} is the proportionality constant of the Hooke's law in three dimensions. It links two second rank tensors so it is a forth rank tensor and it is also symmetric like the other two. This symmetry reduces the number of independent constants, in isotropic solids there are only two independent elastic constants. By Hooke's law and the isotropic form of c_{ijkl}, extensional stress can be written as,

$$T_{ij} = \lambda \left(S_{xx} + S_{yy} + S_{zz} \right) + 2\mu_{ij} S_{ii} \tag{1.29}$$

And the tangential stress,

$$T_{ij} = 2\mu S_{ij} \qquad (i \neq j) \tag{1.30}$$

Young's modulus (Y) is the ratio of axial stress to axial strain which can be expressed using the equations above,

$$Y = \frac{\mu\,(3\lambda+2\mu)}{\lambda+\mu} \tag{1.31}$$

Poisson's ratio (σ) is the ratio of the lateral contraction to the longitudinal extension, again expressed using the equations above,

$$\sigma = \frac{\lambda}{2\,(\lambda+\mu)} \tag{1.32}$$

Bulk modulus or the modulus of compression is given by,

$$K = -\frac{p}{S} \tag{1.33}$$

And compressibility is its reciprocal,

$$\chi = -\frac{1}{V}\left(\frac{\partial V}{\partial p}\right) \tag{1.34}$$

The above two are usually specified as to whether the conditions are adiabatic or isothermal.

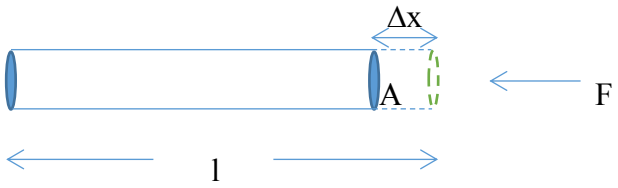

Fig. 1.3: Deformation due to an applied strain

Rigidity modulus or the shear modulus (μ) is the ratio of shear stress to the shear strain.

$$\mu = \frac{F\,l}{A\,\Delta x} \tag{1.35}$$

Just as longitudinal waves are related to the Young's modulus, rigidity modulus plays a role in shear waves.

1.2 Acoustic waves in solids

1.2.1 Phase and Group velocities

Phase velocity is the speed at which a particular phase of any frequency component of a wave travels. So any given phase of a component will travel at the phase velocity. It is expressed as,

$$V_P = \frac{\lambda}{T} = \frac{\omega}{k} \tag{1.36}$$

Where λ is the wavelength of the wave, T is the period, ω is the angular frequency and k is the wave number.

Group velocity of a certain wave is the speed at which the overall shape of the amplitudes of the waves (envelope) propagates. It is written as,

$$V_G = \frac{\partial \omega(k)}{\partial k} \tag{1.37}$$

The function ω(k) is the dispersion relation which relates the frequency to the wave number. If it's a straight line then the group and the phase velocities of the wave are equal. Otherwise the envelope of the wave will take a certain shape and move with the group velocity. This is called the group velocity dispersion. In dispersive media, waves of different frequencies travel at different phase velocities giving rise to a changing pulse shape making the group velocity hard to be defined. When the envelope of the wave packet distorts, different frequency

components move with different speeds meaning faster ones move towards the front and slower ones to the back making the wave packet stretch out.

Group velocity is usually the speed at which the energy is transferred along a wave unless there's absorption in the medium. Group velocity can be zero when the pulse is stopped or negative when it appears to propagate in the opposite direction. However Phase velocity can even be bigger than the speed of light in vacuum.

A difference in amplitude or frequency of a wave with time is called the modulation. It represents the signal content of a wave. Because each amplitude envelope contains a group of internal waves, the speed at which envelopes propagate is called the group velocity. Group velocity can be equal to phase velocity only when the refractive index of a medium is constant. If the phase velocity varies with the frequency, these two differ and this type of a medium is called dispersive.

Group velocity can be derived from the phase velocity by using (1.36) and (1.37) as follows,

$$V_G = \frac{\partial \omega(k)}{\partial k}$$

$$V_G = \frac{1}{\left[\frac{\partial\left(\frac{\omega}{V_P}\right)}{\partial \omega}\right]}$$

$$V_G = \frac{1}{\left(\frac{V_P - \omega \frac{\partial V_P}{\partial \omega}}{V_P^2}\right)}$$

$$V_G = \frac{V_P^2}{V_P - \omega \frac{dV_P}{d\omega}} \tag{1.38}$$

1.2.2 Reflection and transmission of ultrasonic waves at interfaces

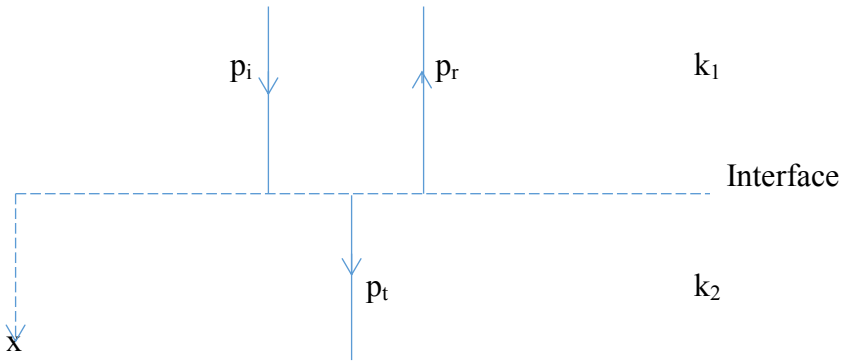

Fig. 1.4: Reflection and transmission of ultrasonic waves at normal incidence at a well-defined interface

Due to the difference in acoustic properties between the two media partial transmission and reflection occurs. The incident, transmitted and reflected waves can be represented by [1],

$$p_i = A \exp j(\omega t - k_1 x) \tag{1.39}$$

$$p_r = AR_P \exp j(\omega t + k_1 x) \tag{1.40}$$

$$p_t = AT_P \exp j(\omega t - k_2 x) \tag{1.41}$$

Where,

R_p – Pressure reflection coefficient

T_p – Pressure transmission coefficient

By the definition of acoustic impedance, the pressure transmission and reflection coefficients for normal incidence can be written as [1],

$$T_p = \frac{2Z_2}{Z_1 + Z_2} \tag{1.42}$$

$$R_p = \frac{Z_2 - Z_1}{Z_1 + Z_2} \tag{1.43}$$

where Z_1 and Z_2 are characteristic acoustic impedances of the two media.

In terms of pressure,

$$R_p = \frac{p_r}{p_i} \tag{1.44}$$

$$T_p = \frac{p_t}{p_i} \tag{1.45}$$

Intensity transmission coefficients are given by,

$$\frac{I_t}{I_i} = \frac{Z_1}{Z_2} \left|T_p\right|^2 \tag{1.46}$$

$$\frac{I_r}{I_i} = \left|R_p\right|^2 \tag{1.47}$$

Using this it can be shown that the law of conservation of energy is satisfied,

$$I_i = I_r + I_t \tag{1.48}$$

The transmitted intensity is symmetric with respect to the incident medium whereas pressure and particle velocity are not.

1.2.3 Acoustical Standing Waves

Two waves with same frequency and mode but travelling in opposite directions cause standing waves. This static pattern of nodes and antinodes has no propagation of energy. Formation of standing waves is due to the total reflection of the plane wave at a perfectly reflecting interface. At the rigid boundary there is a displacement node and a pressure anti-node. It's the opposite if there is a free surface or interface. Now the pressure is the total of the incident and reflected wave [1].

$$P = p_i + p_r \tag{1.49}$$

which gives,

$$p = e^{i\omega t}\left(1 + R_p\right)\cos kx - \left(1 - R_p\right) i \sin kx \; e^{i\omega t} \tag{1.50}$$

At rigid boundaries ($R_p = 1$),

$$p = 2\cos kx \; e^{i\omega t} \tag{1.51}$$

At free surfaces ($R_p = -1$),

$$p = 2\sin kx \; e^{j(\omega t - \pi/2)} \tag{1.52}$$

Travelling waves are usually a propagation of a disturbance and take the form f(ωt – kx) = 0 and standing waves take the form f(ωt) g(kx) which shows that the spatial and temporal form are separated. This helps categorizing free and standing waves. However if the reflection coefficient is not unity the amplitudes at the nodes are no longer zero. This is called standing wave ratio (SWR) as it's a mix of a standing wave and a traveling wave and is given by,

$$SWR = \frac{p_{antinode}}{p_{node}} \equiv \frac{1 + R_p}{1 - R_p} \tag{1.53}$$

The power flow can be described by the acoustic Poynting vector, the acoustic power per unit area transmitted across a surface.

$$\vec{I} = \overline{p(t)\, v(t)} = \frac{1}{2}\, Re\, (pv^*) \tag{1.54}$$

where v^* is the particle velocity.

For standing waves the particle displacement and velocity are in phase. Average acoustic intensity is zero meaning that there is no propagation of acoustic energy.

CHAPTER 2

ACOUSTIC WAVES IN BOUNDED MEDIA

Important physical features of the modes of propagation are frequency dependence of phase velocities, group velocities, displacement distributions, mode coupling and selective attenuation.

Vector differential equation for small elastic motions in an elastic isotropic medium can be written as [2],

$$\mu\nabla^2 u + (\lambda + \mu)\nabla(\nabla . u) = \rho \frac{\partial^2 u}{\partial t^2} \tag{2.1}$$

where,

u – displacement vector

Solutions to (2.1) can be formed from vector potential function (ψ) and scalar potential function (φ) such that,

$$u = \nabla\varphi + (\nabla \times \psi) \tag{2.2}$$

Velocity of a longitudinal wave (V_L) and a shear wave (V_S) in an infinite elastic medium can be obtained by substituting (2.2) into (2.1),

$$V_L = \sqrt{\frac{\lambda+2\mu}{\rho}} \tag{2.3}$$

$$V_S = \sqrt{\frac{\mu}{\rho}} \tag{2.4}$$

A plate of thickness 2b (bounded by planes at x = ±b) and infinite along y and z is considered. When elastic properties are not specified in terms of λ and μ, frequency equations can be written using V_S, Poisson's ratio σ, dimensionless angular frequency $\omega b/V_S$ and dimensionless propagation constant γb. The solutions to frequency equations are usually in the form of a series of continuous curves or branches. For a given mode of propagation there is a branch relating the dimensionless frequency and the propagation constant. Then the dimensionless phase velocity can be defined as $(\omega b/V_S)/\gamma b$ and similarly the group velocity. This group velocity is related to the slope of the mode curve. The cut off frequency of a mode is the lowest frequency at which free propagation can occur. In other words, it is the lowest frequency that the propagation constant would have a real value for a given mode. Usually it is a frequency of zero group velocity or zero propagation constant. Modes can be classified as four families, longitudinal, flexural, symmetrical shear and anti-symmetrical shear. In shear waves or SH waves the displacement is transverse to the direction of propagation. In longitudinal modes particle displacement vectors are symmetrically arranged with respect to the median plane whereas they are anti-symmetrically arranged in flexural modes.

2.1 SH modes

2.1.1 Symmetric (s) and anti-symmetric (a) SH modes

Fig. 2.1: Plate vibration of symmetric (left) and anti-symmetric (right) modes

The lowest anti-symmetrical SH mode is designated as a_o and the lowest symmetric SH mode s_o. For all a and s modes, the phase and group velocities are functions of frequency which tells that they are dispersive modes of propagation. For imaginary propagation constants, displacements decay exponentially in z while for real γb, displacements are sinusoidal. The decay is not due to losses in the medium and rather because energy being stored in space and not propagating freely. Another explanation is that the stress and particle velocity are 90^0 out of phase making energy flux zero.

For s_o mode, $\gamma b = \omega b/V_S$, resulting in the group and phase velocities being independent of frequency and therefore being the only non-dispersive SH mode. Only one elastic constant, the shear modulus, is involved in SH modes whereas two are involved in longitudinal and flexural modes. For a given frequency a finite number of freely propagating SH modes occur, which are the solutions in real γb of the frequency spectrum. In imaginary γb, there are an infinite number of solutions which forms an arbitrary stress distribution. This physically means an arbitrary SH excitation of a plate results in having elastic energy stored in non-propagating modes and elastic energy travel into the plate in propagating modes.

2.1.2 Waveguide equation for SH modes

There is only one direction of polarization in SH modes and they are decoupled from the other modes, so there is no mode conversion or reflection. The displacement is perpendicular to the plane of the plate. The principle of transverse resonance states that resonance occurs at multiples of λ/2, which can be written as [1],

$$\frac{n\lambda}{2} = b \tag{2.5}$$

Where,

n - an integer

λ - wavelength

b - plate thickness

Then the transverse wave number k_t can be written as,

$$k_t = \frac{\pi n}{b} \tag{2.6}$$

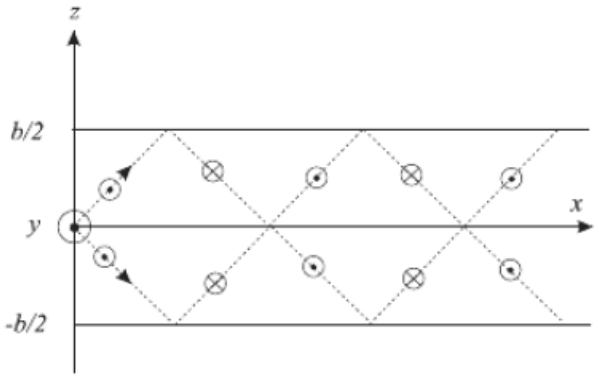

Fig. 2.2: Partial waves of SH modes used for guided wave analysis [1]

As shown in figure 2.2, incident and reflected waves have a wave vector γ in the propagation direction. From this, the waveguide equation can be obtained as,

$$\gamma^2 = \left(\frac{\omega}{V_S}\right)^2 - \left(\frac{n\pi}{b}\right)^2 \quad (2.7)$$

Where,

V_S - Shear wave velocity

ω – Angular frequency

In a waveguide as the frequency is increased, the transverse component of a given mode decreases. For frequencies below transverse resonance frequency, the partial waves move off the slowness curve and γ becomes imaginary making the wave evanescent or non-propagating. At transverse resonances for even modes, there is even symmetry (symmetric mode) about the median plane whereas there is odd symmetry (anti-symmetric mode) for odd modes.

2.2 Lamb Waves

Lamb waves are elastic waves that propagate in solids whose particle motion lies in the plane containing the direction of propagation and the plate normal. Solid plates support two infinite sets of modes whose velocities depend on the wavelength and the plate thickness. Lamb waves are constrained by the elastic properties of the plate or surface they are guided by. Lamb waves have practical application mainly in non-destructive testing of materials.

In Lamb waves the partial wave modes are composed of longitudinal and transverse components in the sagittal plane. Unlike Rayleigh waves, Lamb waves occur in a plate having a

finite thickness. Lamb waves are dispersive, so the phase and group velocities vary with frequency. Velocity fields of incident and reflected partial waves are defined as [1],

$$v_{li} = A_l e^{-jk_{li}.\vec{r}}$$

$$v_{lr} = B_l e^{-jk_{lr}.\vec{r}} \quad (2.8)$$

$$v_{si} = A_s e^{-jk_{si}.\vec{r}}$$

$$v_{sr} = B_s e^{-jk_{sr}.\vec{r}}$$

Where,

'v' s are the velocity fields, 'A' s and 'B' s are the amplitudes, l and s refer to longitudinal and shear waves respectively and i and r refer to incident and reflected waves.

2.2.1 Longitudinal and flexural modes

There are two families of waves, one whose motion is symmetrical about the mid plane of the plate and the other whose motion is anti-symmetric about the mid plane of the plate, as shown in figure 2.3. In the low frequency range the zero order modes of these are called the extensional mode and the flexural mode respectively. The elliptical particle motion for the symmetrical extensional mode is mainly in the plane of the plate whereas it is perpendicular to the plane of the plate in the asymmetric flexural mode. The extensional mode usually has a higher velocity and a lower amplitude whereas the flexural mode is more easily excited and often carries most of the energy. These two modes exist at all frequencies and carry more energy than higher order modes in most practical situations.

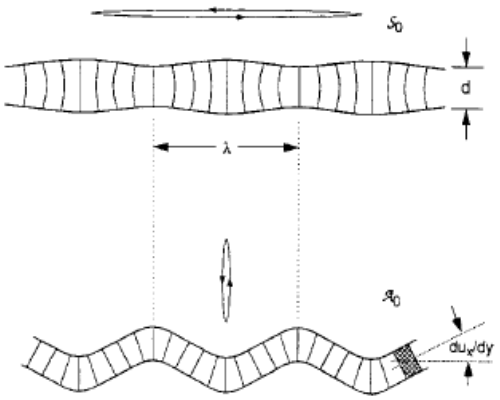

Fig. 2.3: Deformation of particle planes and retrograde elliptical motion at the plate surface of symmetric (top) and anti-symmetric (bottom) modes of Lamb waves [1]

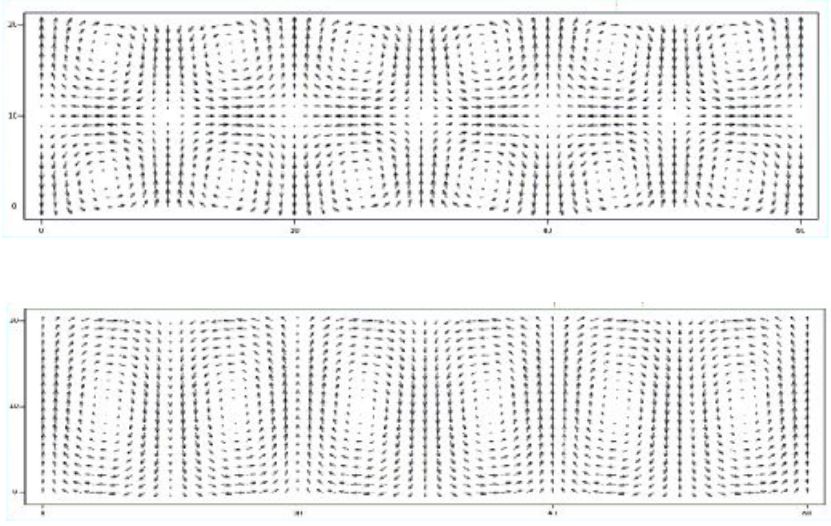

Symmetric

Anti-symmetric

Fig. 2.4: The actual particle motion, shown in arrows, of symmetric (top) and anti-symmetric (bottom) Lamb wave modes

At low frequencies the zero order symmetrical mode or the extensional mode as it is called, propagates at the plate velocity with the plate stretching in the direction of propagation and contracting correspondingly in the perpendicular direction. As the frequency increases (when

the wavelength becomes comparable to the plate thickness), the phase velocity drops smoothly while the group velocity drops steeply and at high frequencies they converge towards the Rayleigh wave velocity.

The zero order anti-symmetric mode, also called the flexural mode, is highly dispersive at low frequencies. At these frequencies for very thin plates, the phase and group velocities are proportional to the square root of the frequency and the group velocity is twice the phase velocity. At higher frequencies these are not valid and the phase velocity rises slowly and converges towards the Rayleigh wave velocity while the group velocity goes through a maximum before converging towards the Rayleigh wave velocity.

Longitudinal modes are specified as L(p) and flexural modes as F(q), where L(0) and F(0) would be the lowest longitudinal and flexural modes respectively. Frequency equations for these modes are given by the Rayleigh-Lamb frequency equations.

For longitudinal modes [1,2],

$$\frac{\tan \beta b}{\tan \alpha b} = -\frac{4(\gamma b)^2(\beta b)(\alpha b)}{[(\gamma b)^2-(\beta b)^2]^2} \tag{2.9}$$

For flexural modes,

$$\frac{\tan \beta b}{\tan \alpha b} = -\frac{[(\gamma b)^2-(\beta b)^2]^2}{4(\gamma b)^2(\beta b)(\alpha b)} \tag{2.10}$$

where α and β are constants.

By solving these equations for group and phase velocities in terms of the frequency, dispersion curves for a specific material can be obtained. These are transcendental equations and can only be simplified as far as,

$$V_L(2V_S^2 - V_P^2)^2 \tan\left(2\pi bf\sqrt{\frac{1}{V_S^2} - \frac{1}{V_P^2}}\right) +$$

$$4V_S^3\sqrt{(V_P^2 - V_L^2)(V_P^2 - V_S^2)} \tan\left(2\pi bf\sqrt{\frac{1}{V_L^2} - \frac{1}{V_P^2}}\right) = 0 \qquad (2.11)$$

Where,

V_P – phase velocity

V_L – longitudinal velocity

f – frequency

Traction free boundaries of the plate couple uncoupled shear waves (SV) and longitudinal waves (L). Partial conversion from one type to another occurs upon reflection at a free surface whereas in shear waves it doesn't. There are symmetric and anti-symmetric displacements though, just like in SH waves. If coupling did not occur, circles, ellipses, hyperbolae and lines of the frequency spectrum would be characteristic in wave motions in plates.

Among the phase velocities, Rayleigh velocity (V_R) is the high frequency limiting velocity for both first longitudinal and first flexural modes in a plate. It can be obtained in terms of elastic parameters using [2],

$$\left(\frac{V_R^2}{V_S^2}\right)^3 - 8\left(\frac{V_R^2}{V_S^2}\right)^2 + 24\left(\frac{V_R^2}{V_S^2}\right) - 16\left(\frac{V_R^2}{V_L^2}\right) + 16\left(\frac{V_S^2}{V_L^2}\right) - 16 = 0 \qquad (2.12)$$

Then the Lame velocity (V_{Lm}) is the velocity of pure SV waves in plates. This can be expressed as,

$$V_{Lm} = \sqrt{\frac{2\mu}{\rho}} = \sqrt{2}\, V_S \qquad (2.13)$$

Plate velocity (V_P) is the low frequency limiting velocity in the first longitudinal mode which is given as,

$$V_P = V_S\sqrt{\frac{2}{1-\sigma}} \tag{2.14}$$

There are two ways to present dispersion curves of plate waves. The first one uses phase velocity along the y-axis and the product of frequency and plate thickness along the x-axis as shown in figure 2.5. The second approach uses the dimensionless parameters $\frac{\omega b}{\pi V_t}$ along the y-axis and βb along the x-axis as shown in figure 2.6.

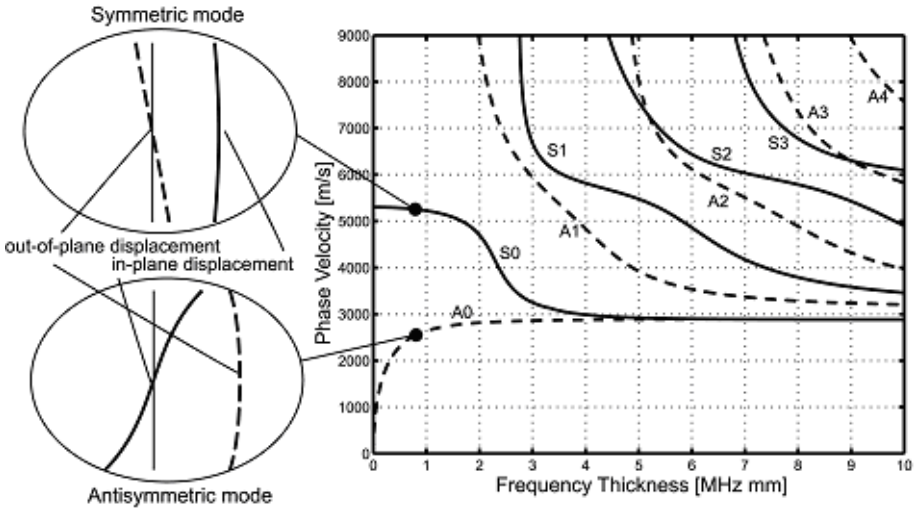

Fig. 2.5: Phase velocities of Lamb wave modes in an aluminium plate as a function of frequency x thickness of plate [10]

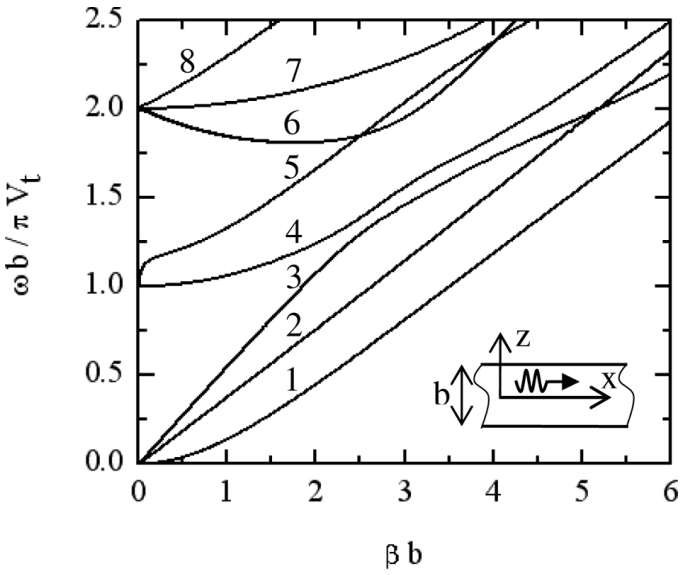

Fig. 2.6: Frequency spectrum of PAW in lithium niobate plotted against a dimensionless parameter (here $V_t = V_S$ and β = wave vector) [4]

2.3 Partial wave analysis

The potential method can only be used for isotropic materials, but as most acoustic waveguides are made out of anisotropic materials, partial wave analysis comes in handy. The basic idea of the partial wave method is to consider the different components of the plane wave solutions separately. These components or partial waves are usually SH or sagittal wave modes which are oriented in such a way that they have a common wave vector in the direction of propagation. The transverse components of the wave vector are real or imaginary depending on the frequency of the wave. The transverse resonance determines the possible modes in the waveguide leading to low frequency cutoffs and many higher order modes. Along with the partial wave method and transverse resonance, slowness curves are also useful in describing waveguide applications.

2.4 Rayleigh waves

Rayleigh waves are a type of surface acoustic wave travelling through solids. They are guided to propagate confined to within approximately a single wavelength, along a surface. The longitudinal and shear motions are coupled together in Rayleigh Waves and they travel at a common velocity but there is a phase difference between these two component motions. As the distance from the surface to the propagation layer increases, the amplitude decreases as the inverse square root of the radial distance from the surface. Rayleigh waves are produced in various ways such as localized impacts, piezoelectric transduction and by earthquakes. In isotropic solids, Rayleigh waves cause surface particles to move elliptically in planes perpendicular to the surface and parallel to the direction of propagation. At shallow depths from the surface this motion is retrograde. Rayleigh waves have a speed slightly less than shear waves depending on the elastic properties of the material.

Rayleigh waves are used in modern microelectronics in the form of filters, delay lines, inter-digital transducers and in many electro-acoustic functions. They are also used in non-destructive testing for detecting defects. Also, in seismology these are the most important type of surface waves.

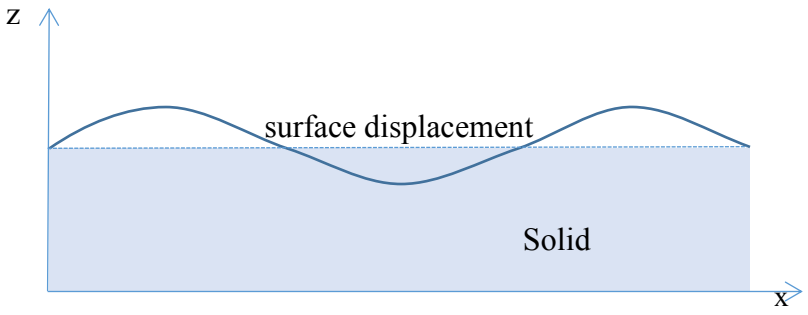

Fig. 2.7: Displacement of the surface of a plate due to Rayleigh wave propagation

Shown above is a wave propagating in the x direction along a surface which has a normal in the z direction. The displacement and velocity components are in the x and z directions. Just like with bulk waves, scalar and vector potentials are [1],

$$\vec{u} = \vec{\nabla\phi} + \vec{\nabla} \times \vec{\psi} \tag{2.15}$$

where ϕ and ψ are the potentials for longitudinal and transverse wave components respectively. The corresponding wave equations can be written as,

$$\frac{\partial^2\phi}{\partial x^2} + \frac{\partial^2\phi}{\partial z^2} + k_L^2\,\phi = 0 \tag{2.16}$$

$$\frac{\partial^2\psi}{\partial x^2} + \frac{\partial^2\psi}{\partial z^2} + k_S^2\,\psi = 0 \tag{2.17}$$

Where,

$k_L = \sqrt{\frac{\rho}{\lambda+2u}}$ $\qquad$ $k_S = \sqrt{\frac{u}{\rho}}$ $\qquad$ are bulk wave numbers.

As the longitudinal and shear components are coupled together in Rayleigh waves, they have a common wave number. In order to determine the potentials the displacements with z, surface wave velocity and then propagation constant (β) needs to be found. At the free surface (z=0) the normal and tangential stresses are zero. The displacements and stress components take the form,

$$u_x = \frac{\partial\phi}{\partial x} - \frac{\partial\psi}{\partial z} \tag{2.18}$$

$$u_z = \frac{\partial\phi}{\partial z} + \frac{\partial\psi}{\partial x} \tag{2.19}$$

$$T_{zz} = \lambda\left(\frac{\partial^2\varphi}{\partial x^2} + \frac{\partial^2\varphi}{\partial z^2}\right) + 2\mu\left(\frac{\partial^2\varphi}{\partial x^2} - \frac{\partial^2\psi}{\partial x\partial z}\right) \tag{2.20}$$

$$T_{xz} = \mu\left(\frac{\partial^2\phi}{\partial x^2} + 2\frac{\partial^2\varphi}{\partial x \partial z} - \frac{\partial^2\psi}{\partial x^2}\right) \quad (2.21)$$

Then the potentials become,

$$\phi = A\exp j(\omega t - \beta x - \gamma_L z) \quad (2.22)$$

$$\psi = -j\exp j(\omega t - \beta x - \gamma_S z) \quad (2.23)$$

Where,

$$\gamma_L^2 = \beta^2 - k_L^2$$

$$\gamma_S^2 = \beta^2 - k_S^2$$

are the variations of displacements with z.

Then from characteristic equation,

$$4\beta^2\gamma_L\gamma_S - (\beta^2 + \gamma_S^2)^2 = 0 \quad (2.24)$$

Then the Rayleigh equation can be written,

$$\eta^6 - 8\eta^4 + 8(3 - 2\xi^2)\eta^2 - 16(1 - \xi^2) = 0 \quad (2.25)$$

Where,

$$\eta = \frac{k_S}{\beta}$$

$$\xi = \frac{k_L}{k_S}$$

The waves travel along a layer of thickness approximately in the order of one wavelength because both components have a decay constant similar to Rayleigh wavelength. Surface

particles move elliptically because the two components are in phase. Displacements even at the surface are tiny and with depth, power of the wave decreases rapidly.

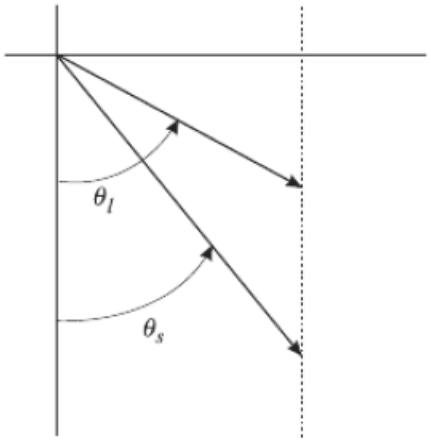

Fig. 2.8: Configuration for partial wave analysis of Rayleigh waves [1]

In a sufficiently thick plate, Rayleigh wave solution can be obtained by considering partial waves for one of the two surfaces. Transverse resonance condition for Rayleigh waves can be obtained as,

$$\sin 2\theta_S \sin 2\theta_l + \left(\frac{V_L}{V_S}\right) \cos^2 2\theta_S = 0 \tag{2.26}$$

Where,

V_S – Shear wave velocity

V_L – Longitudinal wave velocity

Then the dispersion equation can be written as,

$$4\beta_R^2 \alpha_{ts} \alpha_{tl} = (\alpha_{ts}^2 + \beta_R^2)^2 \tag{2.27}$$

2.5 Love waves

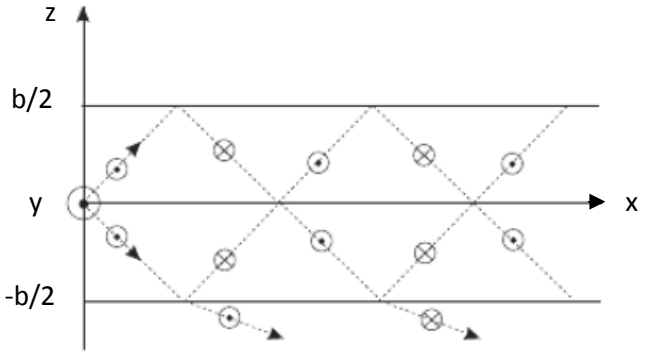

Fig. 2.9: Love waves in a semi-infinite substrate [1]

In isotropic media, SH modes are not coupled with sagittal modes. Love waves are these horizontally polarized shear waves guided by an elastic layer. For a shear wave mode to be trapped in a layer, shear wave velocity in the layer should be lesser than that of the substrate. The partial waves in the substrate are [1],

$$v_{yi} = A \exp -j(-\hat{k}_{ts}z + \beta x)$$

$$v_{yr} = B \exp -j(\hat{k}_{ts}z + \beta x) \quad (2.28)$$

$$v_{yt} = C \exp -j(\hat{k}_{ts}z + \beta x)$$

Where i, r and t refer to incident, reflected and transmitted respectively and A, B and C are constants.

In a plate at low frequencies, phase velocity of Love waves tends to the wave velocity in the substrate due to the high wavelength compared to the layer thickness. At high frequencies, Love modes behave as bulk shear waves in the layer and the phase velocity approaches the bulk

shear velocity. Also they penetrate deep in to the substrate at low frequencies but are confined to the layer as frequency increases.

In Love waves, because of the finite thickness of the layer there is a finite length scale of wavelength making them dispersive. Further the nature of the modes depends on the layer to substrate ratios. To obtain the nature of the modes, partial wave analysis and the waveguide equation with transverse resonance are used.

The layer is said to stiffen the substrate when the shear wave velocity in the layer is higher than in the substrate. For vanishing layer thicknesses, the velocity is the Rayleigh wave velocity for the substrate. For higher thicknesses the partial wave leaks into the substrate making the mode a pseudo bulk wave.

The layer is said to be loading the substrate when the shear wave velocity in the layer is lesser than in the substrate. When the layer thickness increases, the velocity decreases due to the effect of the low velocity material. When the layer thickness is infinite the velocity approaches the Rayleigh velocity. Here Rayleigh modes are excited because of transverse resonance as much as Love waves. At low frequencies these leak into the substrate. The lowest of the Rayleigh modes is useful in seismology and device physics.

2.6 Stoneley waves

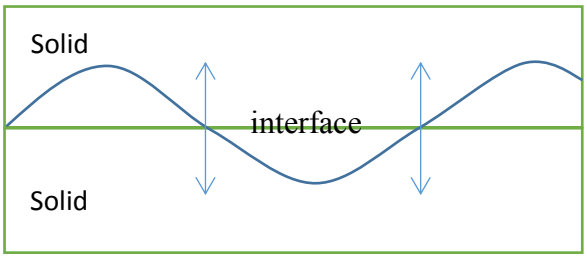

Fig. 2.10: Stoneley wave propagation along a boundary in between two solids

A Stoneley wave is a wave propagating along the interface between two solids that is also evanescent in both media. The intensity of the wave decreases as you go away from the interface. Stoneley wave velocity lies in between the velocities of Rayleigh waves and shear waves. Stoneley waves are useful in estimating rock properties. Permeability can make Stoneley waves be partly reflected at sharp impedance contrasts, change the wave velocity of it inducing dispersion and also cause attenuation.

2.7 Waveguide configurations

Beam spread due to diffraction, having a single orientation, inability to turn corners and the inability to go from one layer device to another are a few reasons that prompted the use of acoustic waveguides. Waveguides suppress the beam spread reducing the width down to an order of a wavelength and the guide can be oriented. It also allows high power densities. When designing a waveguide the degree of field of confinement or the rate of decay of the acoustic field in the substrate is controlled according to the application. Due to the intrinsic length scale involved in the thickness of guides, dispersion usually occurs. Generally a dispersionless or low dispersion bandwidth is designed. There are several different approaches to waveguides.

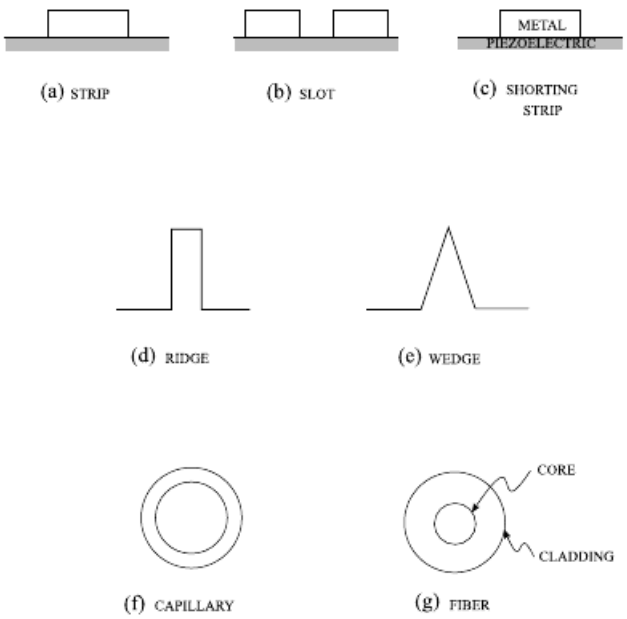

Fig. 2.11: Several acoustic waveguide configurations [1]; (a), (b), and (c) are flat overlay waveguides, (d) and (e) are topographic waveguide configurations and (f) and (g) are two types of circular fiber waveguides

Overlay waveguides have a film or films deposited on the substrate to lower the sound velocity. This can lead to evanescent decay of the mode in the substrate. The material of the overlay is chosen depending on the acoustic loading of the substrate underneath. The strip guide (figure 2.11 (a)) is dispersive and as the frequency increases the wave velocity decreases towards the Rayleigh velocity and the wave becomes confined to the strip.

The slot waveguide guides (figure 2.11 (b)) the wave along the bare substrate with the help of strip on either side. The material is chosen as to stiffen the Rayleigh velocity of the substrate so that the acoustic wave is trapped. The phase velocity increases with frequency and at higher frequencies it is equal to the Rayleigh velocity of the substrate and the acoustic wave is confined to the slot.

Shorting strip waveguides (figure 2.11 (c)) use metallic shorting strips on a piezoelectric substrate. The metal shorts the piezoelectric field which decreases the Rayleigh velocity depending on the magnitude of the piezoelectric constant. Another approach is to use diffusion to create the required velocity changes. Significant velocity changes can be achieved with no rise of attenuation.

Topographic waveguides are produced by a local deformation of the substrate. The binding is strong and vertical reflections occur. A waveguide with a ridge (figure 2.11 (d)) which anti-symmetrical flexural modes go through is highly dispersive. Ultrasonic field is strongest at the top of the ridge but dies away exponentially towards the substrate. A symmetric pseudo-Rayleigh mode through a ridge waveguide has no dispersion. The displacement is due a combination of S_0 and SH modes and propagates down to zero frequency. A wedge waveguide (figure 2.11 (e)) uses an ideal wedge which no length scale making it dispersionless. Mainly flexural modes are excited and are tightly bound to it.

Circular fiber waveguides were originally developed to achieve low loss, low dispersion and long delay lines. Capillary waveguides (figure 2.11 (f)) propagate Rayleigh waves along the inside surface of a capillary. Group velocity is relatively constant over a limited frequency. Cladded acoustic fibers (figure 2.11 (g)) can also be used as waveguides. An acoustic mode can be trapped in the case if the velocity in the cladding is greater than that of the case. Waves can be propagated over long distances and are used in the development of cladded delay lines.

CHAPTER 3

EXPERIMENTAL INVESTIGATION OF PAW IN ELECTRONIC MATERIALS

3.1 Fast Fourier transform (FFT)

Fast Fourier transform is an algorithm that rapidly converts time to frequency and vice versa. It is obtained by decomposing a sequence of values into components of different frequencies. FFT is largely used in digital signal processing. As shown in figure 3.1, the waveform at the top in the time domain is converted to its frequency components at the bottom by the fast Fourier transform.

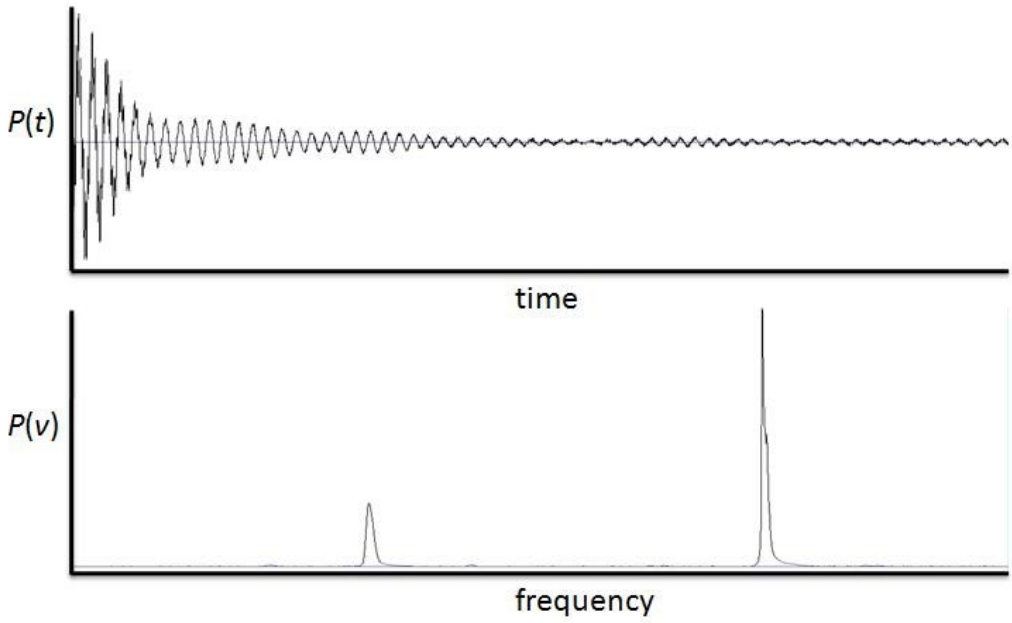

Fig. 3.1: Fast Fourier Transform being applied to a waveform

In the experiments conducted in this project, FFT comes into play in measurements from the oscilloscope. Pulses containing various amounts of bursts (periodic signals) are supplied as the input from the function generator which creates a waveform at the oscilloscope as the output. Both of these waveforms, the input and the output, are observed through the oscilloscope and analyzed using the built in FFT function in the oscilloscope. In the input pulse, the lower the number of bursts you have the more scattered the frequency spectrum of it will be when analyzed by the FFT function. So it is always better to have as high an amount of input bursts as possible without overlapping with the output wave. This will give a frequency spectrum with a sharper peak with the frequencies concentrated in to a narrow range making the actual frequency of the input more accurate. This also avoids exciting the transducer or the crystal with many undesired frequencies. Performing FFT analysis of the output is useful in finding the frequencies of the modes or wave packets in the output waveform. Some images of the FFT performed on lithium niobate are shown later in figures 3.32 and 3.33. It can be seen that more than one frequency peak can be found, and this is due to the excitation of the crystal at those frequencies by resonance. It can also be used to distinguish different modes since they usually have different frequencies.

3.2 Method error (Readout error)

Method error is the experimental error caused by the limitations of precision of the instruments used. It depends on the minimum possible measurement in an instrument and the value measured. If the minimum measurement is m and the value that is being measured is x,

$$Method\ error = \frac{1}{2}\frac{m}{x} \times 100\% \tag{3.1}$$

So the idea is to have the scale of the measurement as large as possible compared to the minimum measurement. In the experiments carried out, this method mostly effects the measurements taken from the oscilloscope. Since the measurements are mainly regarding the delay, the time axis is stretched so that most of the measurement area of the waveform fits in the display. This is doubly advantageous as the points of measurement can be seen larger and precisely. In the following experimental measurements done, it can be seen that the method error ranged from about 1% to about 7% which is reasonable.

3.3 Multi-purpose ultrasonic transducer (ITC-9070-1)

Fig. 3.2: Image of the transducer used for the experiments (white coloured one)

The two transducers used are a transmitting and receiving pair suitable for various applications such as bubble detection, NDT and close range high resolution proximity sensing. Their small size and rugged construction makes them versatile. The specifications of these transducers at 22°C are as shown below. They operate mainly in the 4.5MHz frequency range but can be used effectively in the low frequency regions as well.

Table 3.1: Specifications of the ITC-9070-1 transducer at 22°C

Property	Value	Unit
Frequency	4.5	MHz
Q in Air	18	-
Q in Water	11	-
Capacitance	940	pF
Operating Temperature	-20 - 80	°C
Humidity	0 - 100	%
Weight	2.5	g

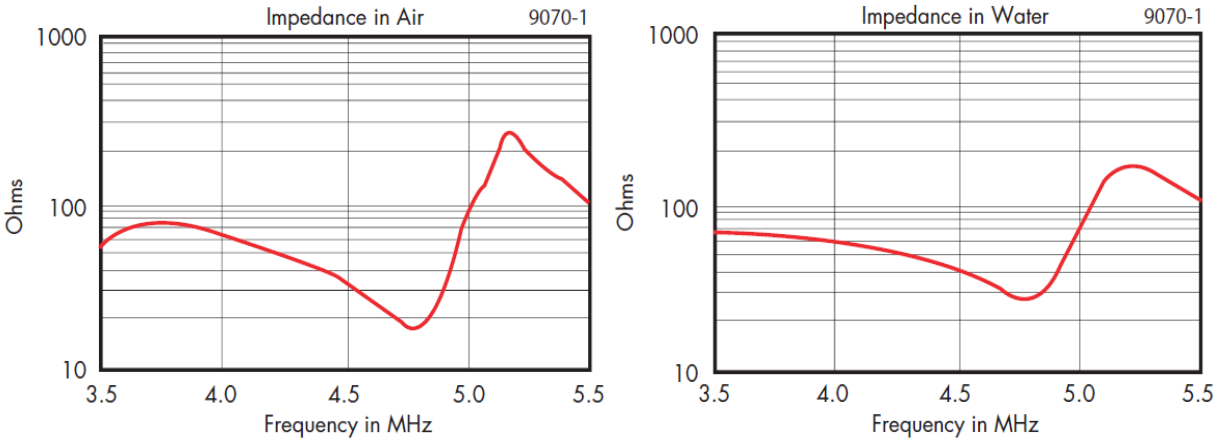

Fig. 3.3: Impedance of the ITC-9070-1 transducer in air and water at different frequencies

3.4 General experimental setup

The general experimental setup used to examine the three materials glass, aluminium and brass is as shown in figure 3.4. The input is provided by an HP 8116A pulse/function generator via a cable connecting it to an ITC-9070-1 multi-purpose ultrasonic transducer. It is also connected to a Tektronix TDS 2014B digital oscilloscope in order to observe the input signal. The digital oscilloscope is triggered externally by the above mentioned function generator via a cable. Output transducer is also connected to the same above mentioned digital oscilloscope to inspect the output waveform. Both of these transducers are grounded at one end. The transducers are attached to the plate with the aid of a layer of Vaseline for the surfaces of the transducers to make good acoustic contact with the plate. The digitally stored information about the input and output waves is then transferred for analysis to a computer via a USB drive.

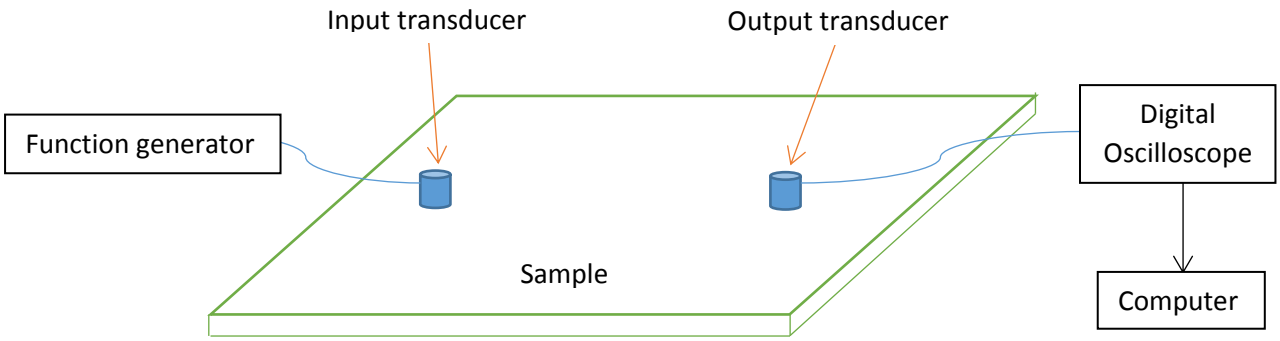

Fig. 3.4: General experimental setup used for the investigation of propagation of acoustic waves through glass, aluminium and brass

3.5 Experimental samples

Different types of plates were used for the investigation of the propagation of Lamb waves through them. The materials used were glass, brass, aluminium and lithium niobate. These plates in general had different lengths, widths and thicknesses. A variety of thicknesses was used for the plates of the same material in order to obtain more experimental points and make the procedure more accurate.

Table 3.2: Samples of plates used for the investigation of propagation of plate acoustic waves

Sample number	Laboratory number	Material	Length (mm)	Width (mm)	Thickness (mm)	Weight (g)	Density (kg/m^3)
1	GL1-S	Glass	75.5	25.45	0.92	8.5	2404.4
2	BR1-S	Brass	268	152	0.07	26.7	9363.4
3	BR2-S	Brass	Irregular	48	0.2	23.8	8838.38
4	BR3-S	Brass	281.5	152	0.3	113.1	8810.88
5	BR4-S	Brass	280	152	0.52	184.6	8341.17
6	BR5-S	Brass	282	98	0.85	195.1	8305.45
7	BR6-S	Brass	302.7	39.2	3.21	328.9	8634.96
8	AL1-S	Aluminium	200	24	4.67	59.6	2658.8
9	AL2-S	Aluminium	126.5	67	3.07	71.1	2732.5
10	AL3-S	Aluminium	229	94	2.45	143	2711.48
11	AL4-S	Aluminium	151	Irregular	1.55	22.4	-
12	LNO-1S	$LiNbO_3$	49	19	1.8	-	-

3.6 Experimental setup for glass

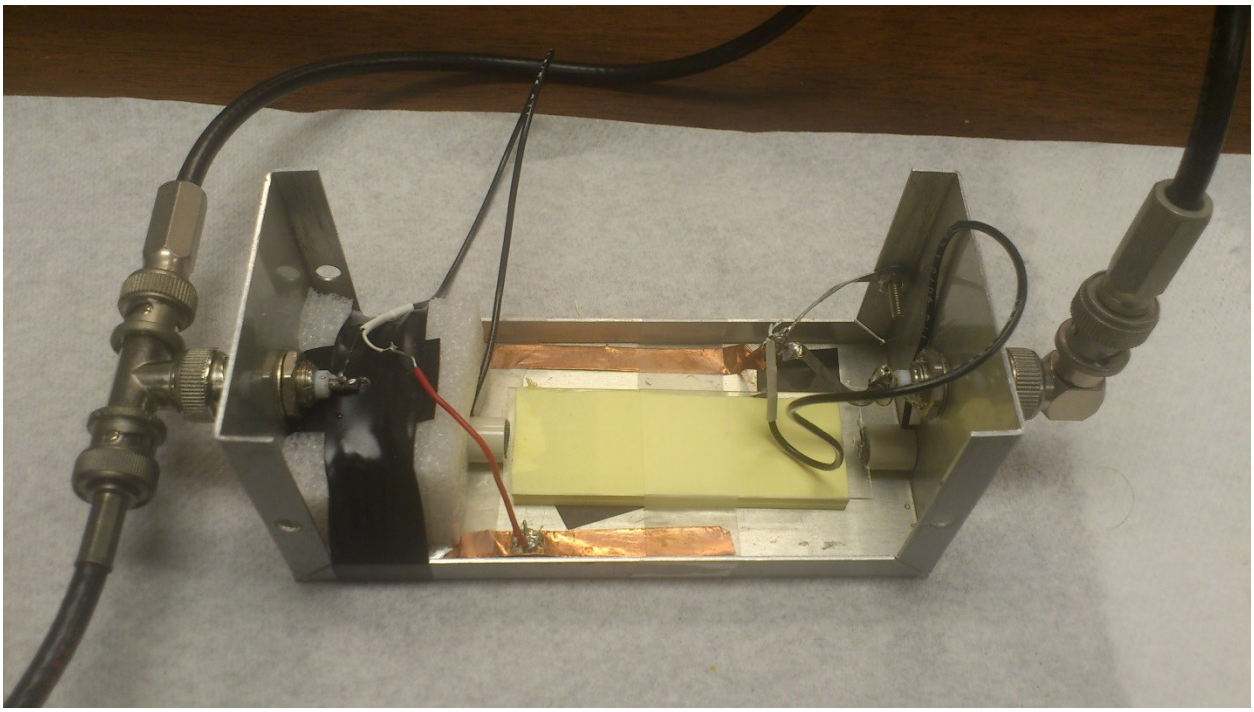

Fig 3.5: Experimental setup for excitation and detection of acoustic waves through a glass plate

The setup for excitation and detection of plate acoustic waves in a glass plate is shown in figure 3.5. The glass plate used here is the same as the glass slides used with microscopes. The dimensions of the glass plate were measured using a digital vernier caliper and a micrometer gauge to be 75.5mm in length, 25.45mm in width and 0.92mm in thickness. The weight of the glass plate was recorded as 8.5g on the Acculab electronic digital scale Model 333, thus giving a density of 2404.18 kg/m^3 which matches with Silicate glass (from glassproperties.com). The acoustic velocities through 'Water white glass' were found to be V_L = 5836 m/s and V_T = 3423 m/s [8] and this was the closest density of a glass variety that matched Silicate glass, so the acoustic velocities were assumed to be similar. This glass plate is taped on to a half open metal box as shown in the figure above at a height which makes it have contact at the center of two

transducers. These transducers are fixed perpendicular to the glass plate in order to propagate acoustic waves along the plate. In between the transducers and the glass plate a layer of Vaseline is applied in order to make good acoustic contact and transfer most of the acoustic waves through the plate rather than air. The transducers used are ITC 90701L93 which have a main operating frequency in the region of 4.5 – 5 MHz. The wire ends of these transducers are soldered to the metal box so that one connects to a function generator and the other to an oscilloscope and are both earthed as well. The metal in the box acts as an earth for the whole circuit. The above mentioned oscilloscope, Tektronix TDS 2014B, is triggered externally by an HP 8116A pulse/function generator through a cable connection. The function generator generates acoustic signal pulses containing sinusoidal waves. The output waveform after the pulse goes through the glass plate is displayed in the oscilloscope. A USB flash drive is plugged in to the oscilloscope to record the data displayed.

3.7 Group velocity of PAW in a glass plate

The function generator produces pulses containing sinusoidal waves of peak to peak voltage of 5V to be propagated through the plate. It is run in internal burst mode producing pulses according to the frequency the transducer is going to be operated at. The duty factor is set at 50% and the pulse width is kept comparatively much smaller than the repetition period in order to avoid overlaps of the waveforms of two consecutive pulses. As the pulses go through the glass plate and to the oscilloscope the output waveform is displayed on its screen. The frequency is varied and the resulting output waveforms are measured by obtaining peaks which generally means the output signal is strong. The signal needs to be comparatively higher than the noise shown in the oscilloscope. For a particular frequency where peaks occur, the wave form in the

oscilloscope is saved and measured. For each of the peaks, by measuring the delay from the start of the original input pulse to the start of the output signal, the group velocities of the modes present can be calculated. Each peak corresponds to a separate mode if there are no reverberations or reflections of the waves from the edges of the plate. Some oscillograms obtained from the oscilloscope for a variety of frequencies are shown in figures 3.6 to 3.9. As seen, the input burst is shown in yellow and the output in green. As the frequency is changed, the speed of the separate modes changes accordingly and can be seen by observing the movement of the peaks, which also vary by strength due to the workable frequencies of the transducers.

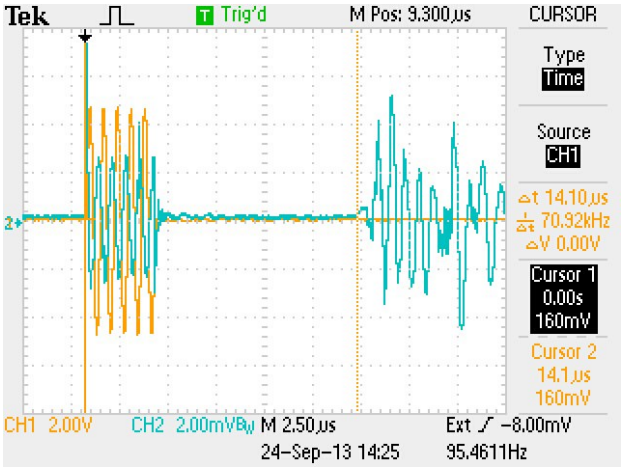

Fig 3.6: Oscillogram containing the acoustic modes propagated through the glass plate and also the air signal at a frequency of 1.44MHz, showing the measurement of delay of the s_o mode using cursors

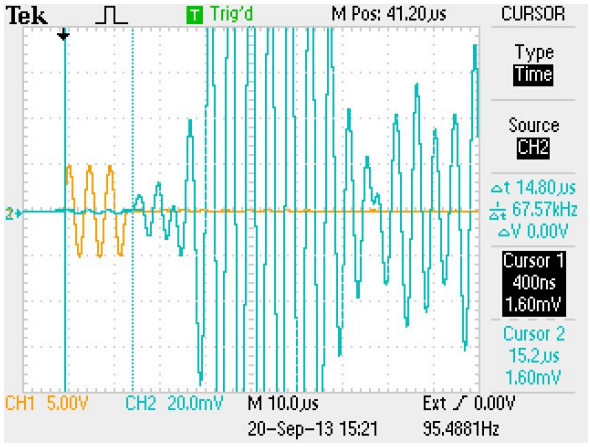

Fig. 3.7: Oscillogram showing the measurement of delay of the s_0 mode at 222kHz

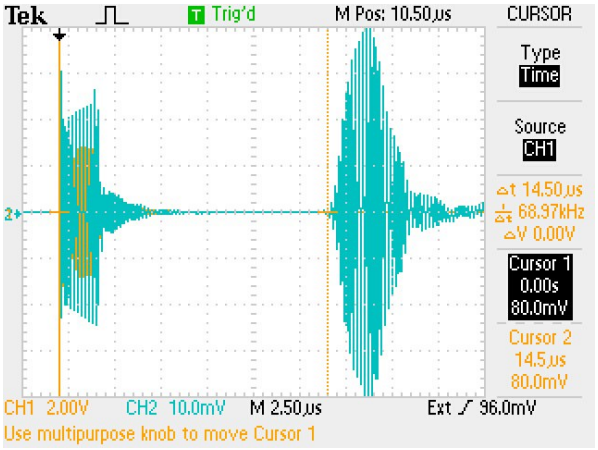

Fig. 3.8: Oscillogram showing the measurement of delay of the s_0 mode at 4.88MHz

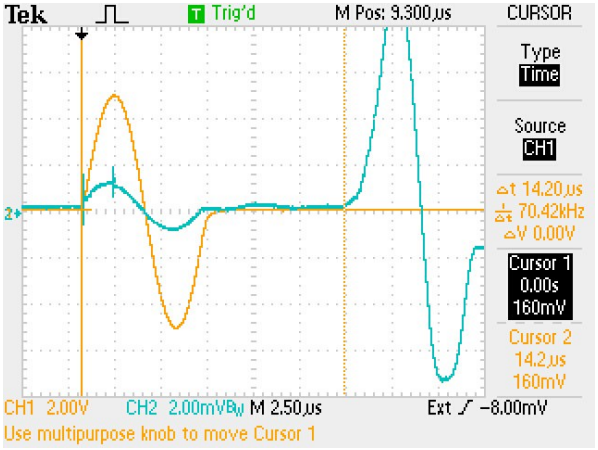

Fig. 3.9: Oscillogram showing the measurement of delay of the s_0 mode at 149kHz

The variation of the delay of couple of modes with the change of frequency is given in table 3.3 below. The thickness of the glass plate was 0.92mm and the distance between the two transducers was 75.5mm. Only the modes a_o and s_o are considered since the curve shown in figure 3.10 [6] contains only those two for comparison. Note that this curve is for a glass plate with V_T = 3200m/s and V_L = 5960m/s and the glass plate used in the experiment has values of V_T = 3423m/s and V_L = 5836m/s, but since the numbers are close enough the comparison can be done with the occurrence of negligible differences.

Table 3.3: Delay of a_0 and s_0 modes propagating through the glass plate at a variety of frequencies

Frequency (MHz)	Delay (μs)	
	a_0	s_0
0.149		14.2
0.169	44.4	
0.233	39.4	
0.480	28.8	
0.819	24.1	14.2
1.09	25.4	
1.41	25.4	
1.44		14.1
2.59	25.2	
2.83		38.2
3.47		33.8
4.91		25.8

Using this set of data the group velocities of each acoustic mode through the glass plate can be calculated using,

$$V_G = \frac{Plate\ length(=75.5mm)}{Delay} \quad (3.2)$$

These calculated group velocities are then compared with the theoretical values as found in the plot (figure 3.10) between frequency x thickness and group velocity [6] by plotting them on the same graph. The Relative velocities are converted to group velocities by multiplying by V_T = 3200m/s.

Table 3.4: Comparison of the experimental points of group velocities with the theoretical values for various frequencies in a glass plate 0.92mm thick

Frequency x 0.92mm (MHz x mm)	Group velocity of a_0 (m/s)			Group velocity of s_0 (m/s)		
	Experimental	Theoretical	Method Error (%)	Experimental	Theoretical	Method Error (%)
0.137				5316.9	5470	1.76
0.155	1700.45		2.25			
0.214	1916.24		1.27			
0.442	2621.53	2880	1.74			
0.753	3132.78	3200	1.04	5316.9	5360	1.76
1.003	2972.44	3220	1.97			
1.297	2972.44	3220	1.97			
1.325				5354.61	5040	1.77
2.383	2996.03	3140	1.98			
2.604				1976.44	1790	1.31
3.192				2233.73	2310	1.48
4.517				2926.36	2850	1.94

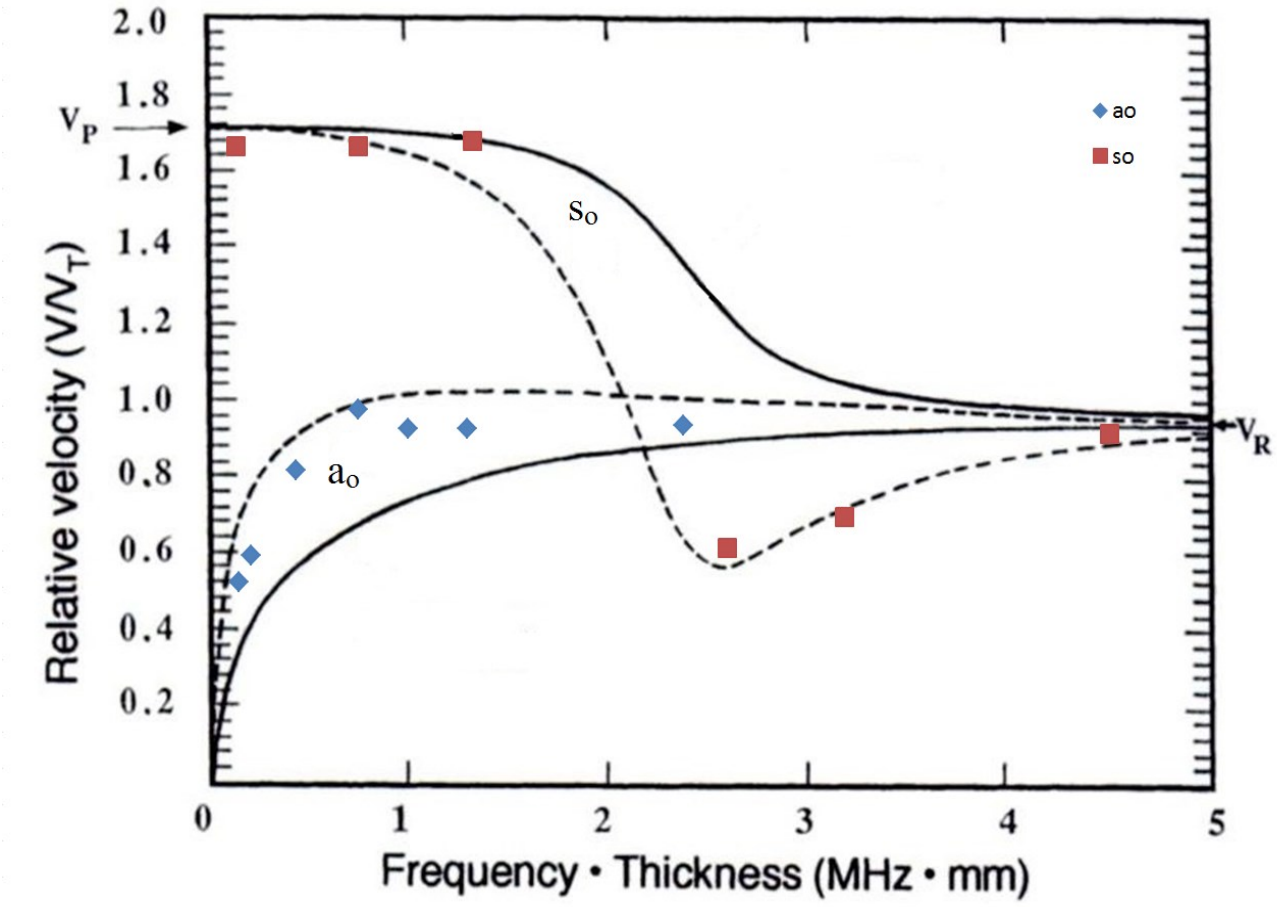

Fig. 3.10: Experimental results (red and blue points) for the group velocity of Lamb waves through a glass plate 0.92mm thick plotted in comparison with theoretical curves of group (- - -) and phase (—) velocities of a_o and s_o modes in a glass plate with V_T = 3200m/s and V_L = 5960m/s from [6]

3.8 Experimental setup for brass and aluminium

To investigate Lamb waves in metal plates, plates of brass and aluminium are being used for propagation of waves through them. A set of metal plates with different thicknesses are tested with two transducers in contact with the surface or edges with the distance between them also

varied. The higher the distance between the transducers is, the better the results will be due to the bigger delay caused making the measurements and the calculations more accurate. There is also some attenuation caused by the plate which is proportional to the square of the frequency of the Lamb waves propagated. The transducers are placed as much towards the center of the surface of the plate as possible in order to lessen the reverberations of the waves caused by the edges of the plate, so the bigger the surface area of the plate the better. These reverberations are caused anyway due to the finite size of the plates but are minimized by the said method as the waves that hit the edges are attenuated by travelling the longer distance and are low in strength and late when reaching the receiving transducer. When transducers are attached perpendicular to the main surface of the plate, the S modes may not be seen because they are longitudinal and would propagate easier if the transducers are attached perpendicular to a side surface of the plate. If the plate is thin it would be hard to fix it parallelly and even if fixed the energy transfer from the transducer to the plate won't be so efficient. Therefore wedges are used to focus the energy from the transducer to the plate. It is better to use lower frequencies and thinner plates since only two modes are encountered then and them too with contrasting velocities so that the peaks can clearly be distinguished in the oscilloscope. The air signal which goes through the air from the input transducer to the output transducer is blocked by placing a grounded metal across the center of the plate just on top of the plate so that the air signal does not interfere with the output wave pattern. It also minimizes the disturbance of the output wave pattern. The plate is placed on some soft sponges so that the waves don't propagate into the metal below it. Also the least amount of cable is used to connect the circuit as they may interfere with the output. The experimental set up for brass plates is shown below in figure 3.11.

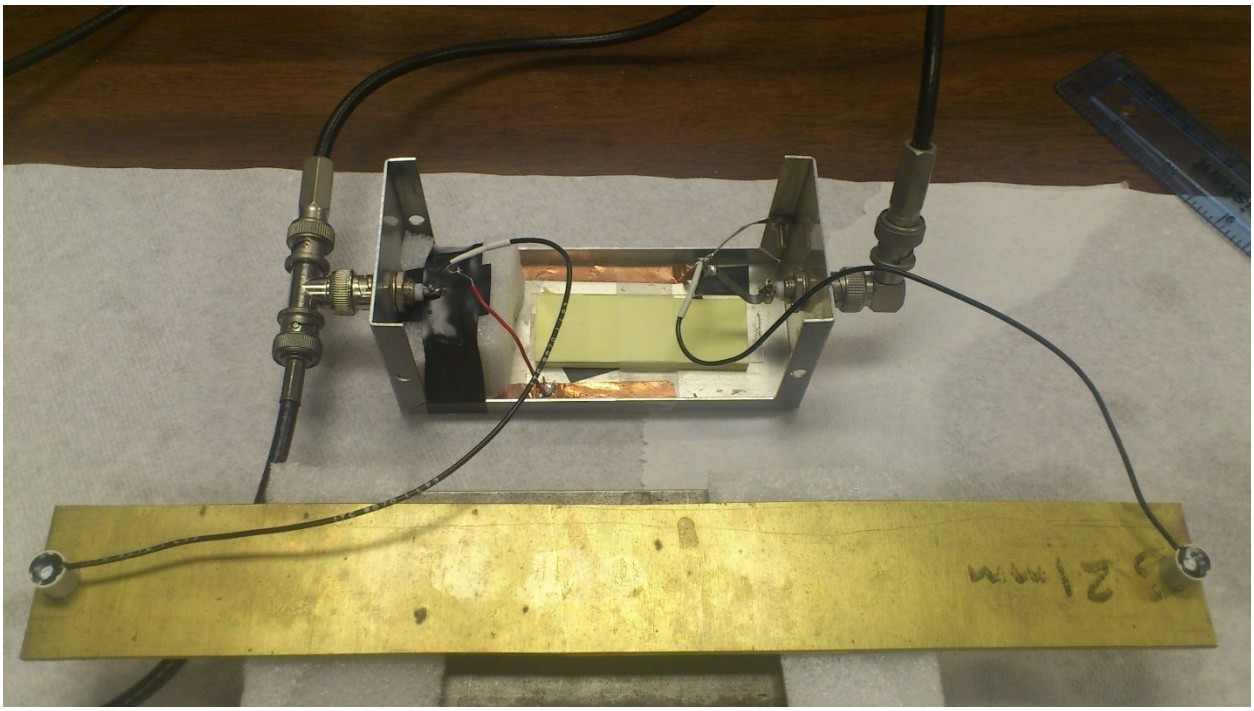

Fig. 3.11: Experimental setup for testing the propagation of PAW through a brass plate of thickness 3.21mm

3.9 Group velocity of PAW in brass samples

Brass was tested with six different samples having various thicknesses. The oscillograms of six measurements from brass plates are shown below in figures 3.12 to 3.17. The input pulse is in yellow and the output waveform is in green. The delay, which is the time difference between the 1st and the 2nd cursors which are also yellow, is displayed again in yellow at the right of each picture as Δt. The data obtained from these are recorded in tables 3.5 and 3.6.

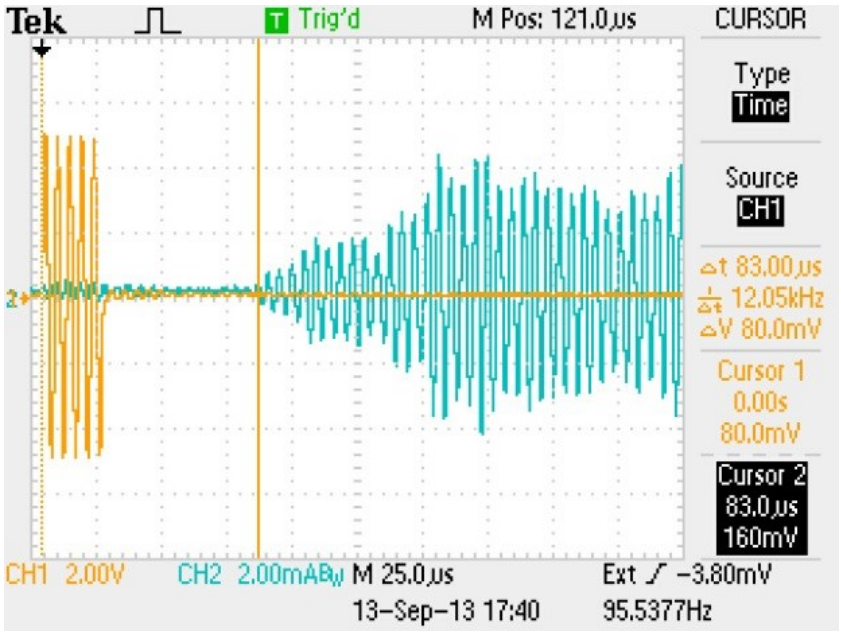

Fig. 3.12: Oscillogram containing some low order acoustic modes propagated through a brass plate 0.07mm thick and also the input pulse at a frequency of 214kHz, showing the measurement of delay of the s_0 mode using cursors

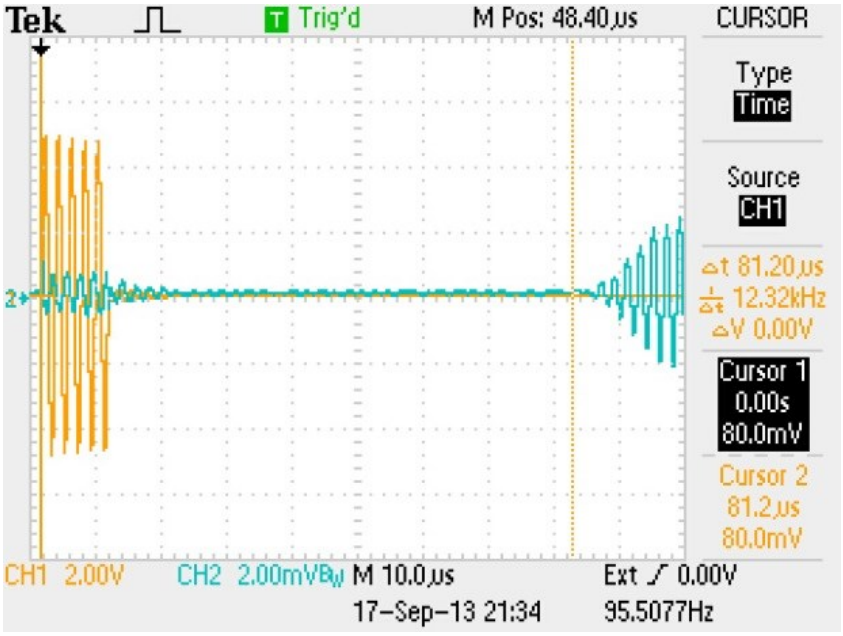

Fig. 3.13: Oscillogram showing the measurement of delay of the s_0 mode propagated through a brass plate 0.3mm thick at a frequency of 495kHz

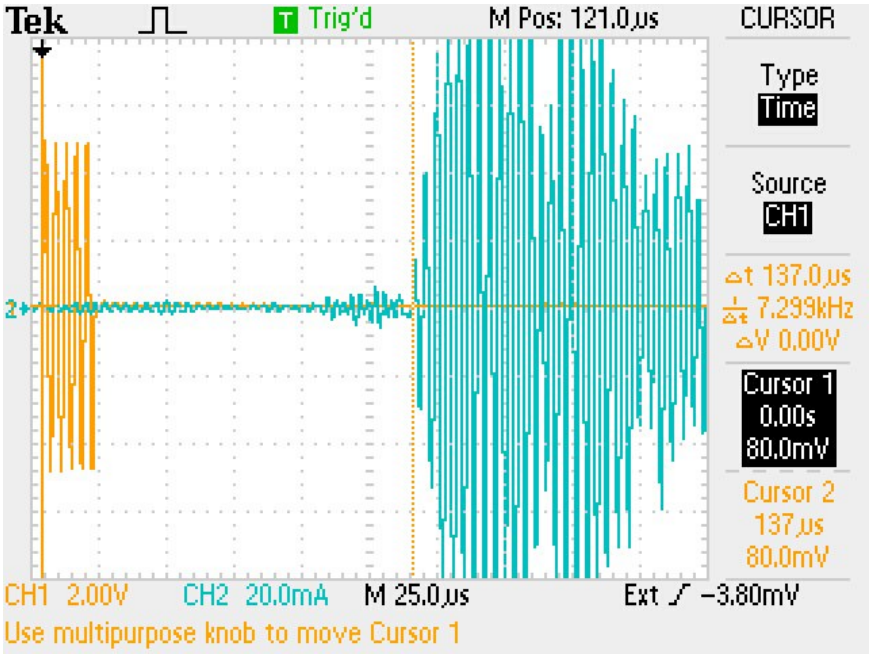

Fig. 3.14: Oscillogram showing the measurement of delay of the a_0 mode propagated through a brass plate 3.21mm thick at a frequency of 260 kHz

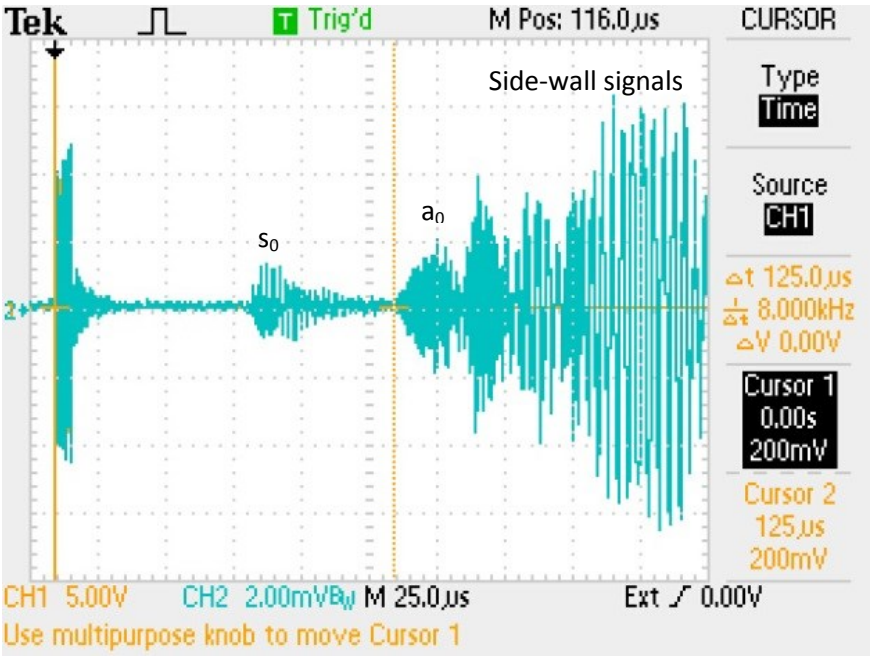

Fig. 3.15: Oscillogram showing the measurement of delay of the a_0 mode propagated through a brass plate 0.52mm thick at a frequency of 825kHz

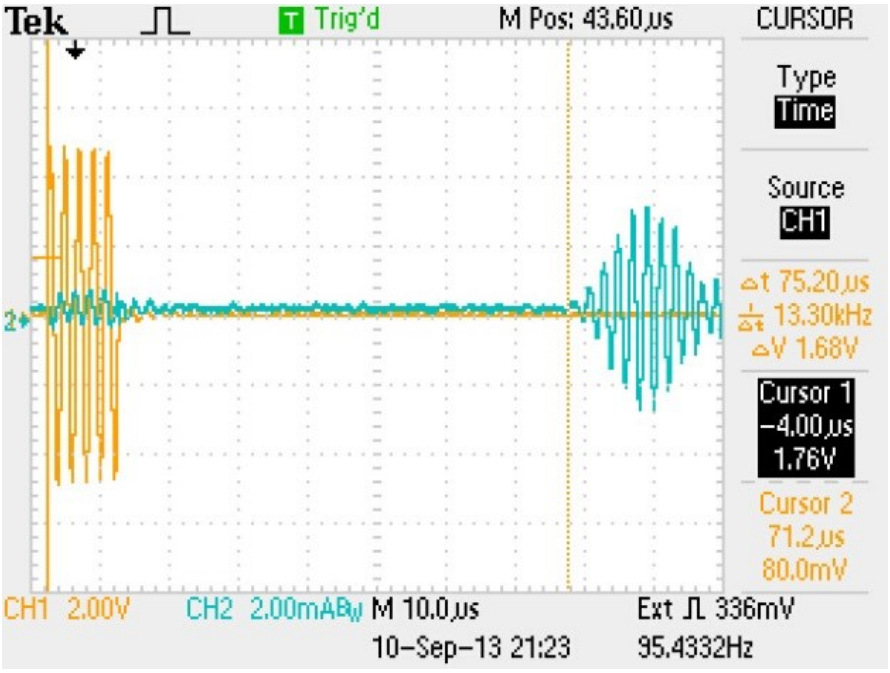

Fig. 3.16: Oscillogram showing the measurement of delay of the s_0 mode propagated through a brass plate 0.85mm thick at a frequency of 486kHz

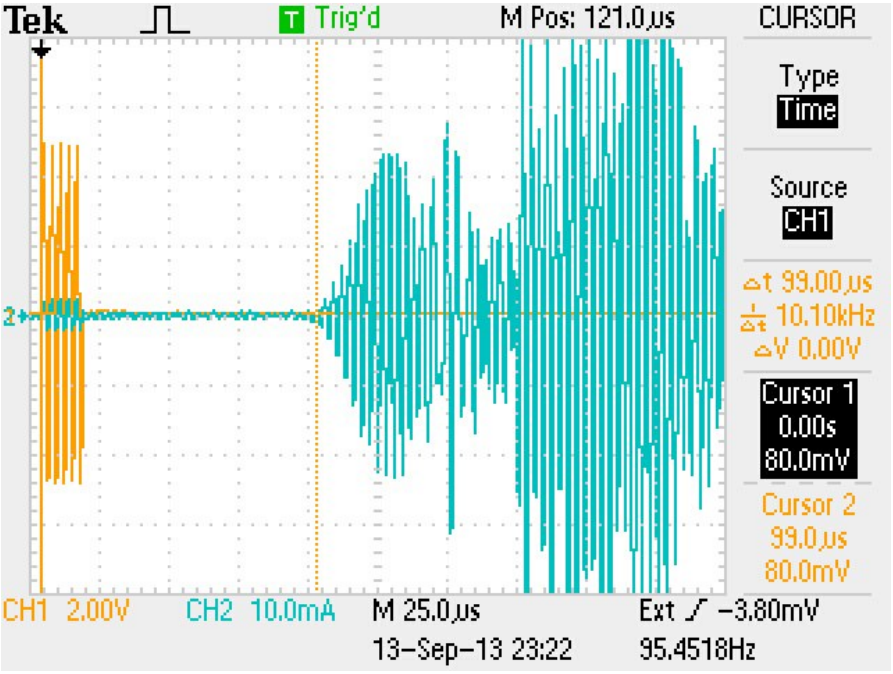

Fig. 3.17: Oscillogram showing the measurement of delay of the s_0 mode propagated through a brass plate 3.21mm thick at a frequency of 339kHz

Table 3.5: Measurements of delays of several propagated acoustic modes in brass plates of different thicknesses for a variety of frequencies

Plate Thickness (mm)	Distance between transducers (mm)	Frequency (kHz)	Delay (μs)		
			a_0	s_0	a_1
0.07	286	123	572		
		214	454	76	
0.2	258	206		73	
		241	233		
		483		69	
0.3	301.5	261		81	
		464	195		
		495		81.2	
		807	164		
0.52	257	203	190		
	295	454		81.2	
	257	500	148		
		825	125		
	295	834		83	
0.85	275.5	115	148		
		433	135		
		486		75.2	
		870		79.2	
3.21	282	63	169		
		206	130		
		260	137		
		339		99	
		475			101

Table 3.6: Group velocities of three separate acoustic modes through brass plates at different frequency-thickness combinations

Frequency x Thickness (MHz x mm)	Group velocity (m/s)	
	a_0	s_0
0.009	500	
0.015	629.96	3723.68
0.041		3534.25
0.048	1107.3	
0.078		3722.22
0.097		3739.13
0.098	1861.49	
0.106	1352.63	
0.139	1538.46	
0.148		3694.58
0.202	1668.64	
0.236		3633
0.242	1829.27	
0.260	1736.49	
0.368	2040.74	
0.413		3663.56
0.429	2056	
0.434		3554.22
0.661	2058.39	
0.739		3478.54
0.835	2058.39	
1.088		2848.48
1.525	a_1 = 2792.08	

These results are compared with the theoretical plot (figure 3.18) shown below. The low frequency x thickness range is then magnified in Figure 3.19 and the experimental points are included. Since only the very low range of frequency x thickness comes into consideration, only the two modes a_0 and s_0 are existent with the a_1 mode coming in to the picture at the very end. Only these three modes are recorded and compared.

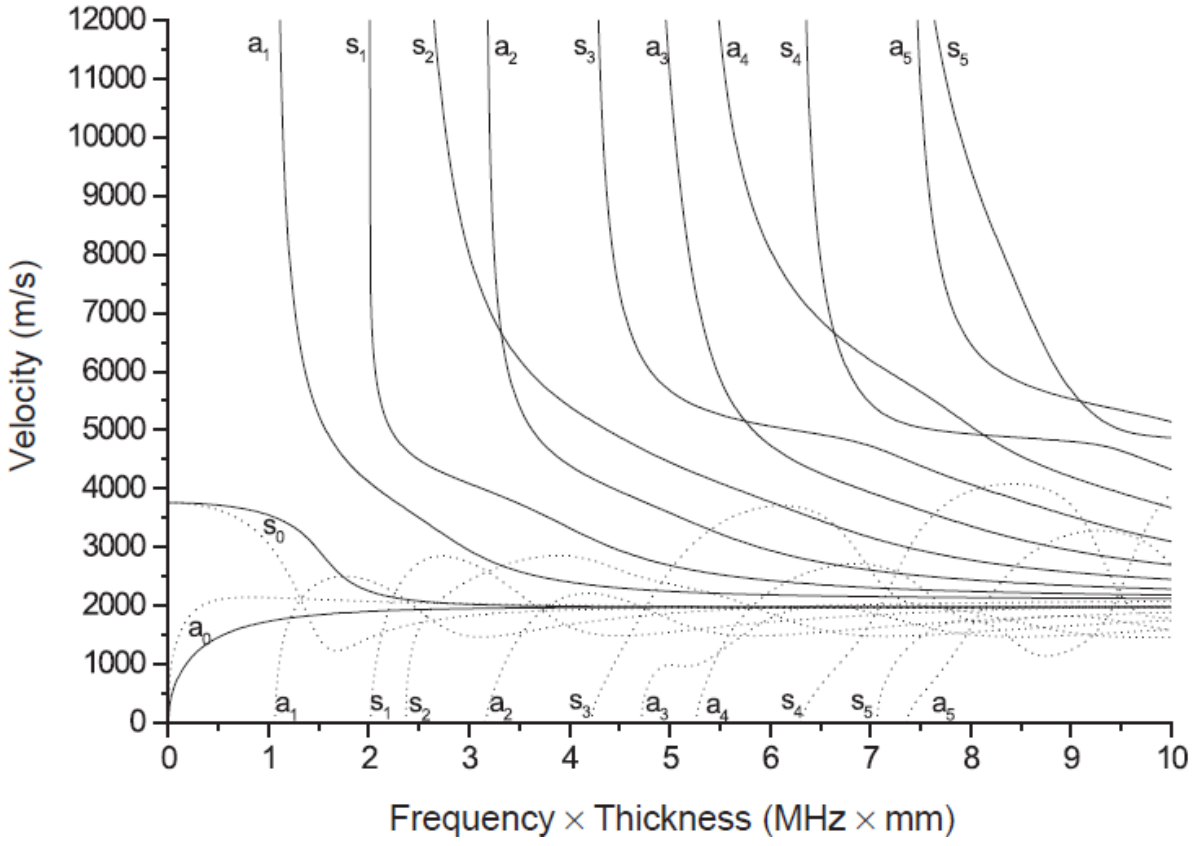

Fig. 3.18: Phase (—) and group (⋯) velocities of plate acoustic waves in a brass plate having V_L = 4700 m/s and V_S = 2100 m/s as a function of frequency x thickness from [1]

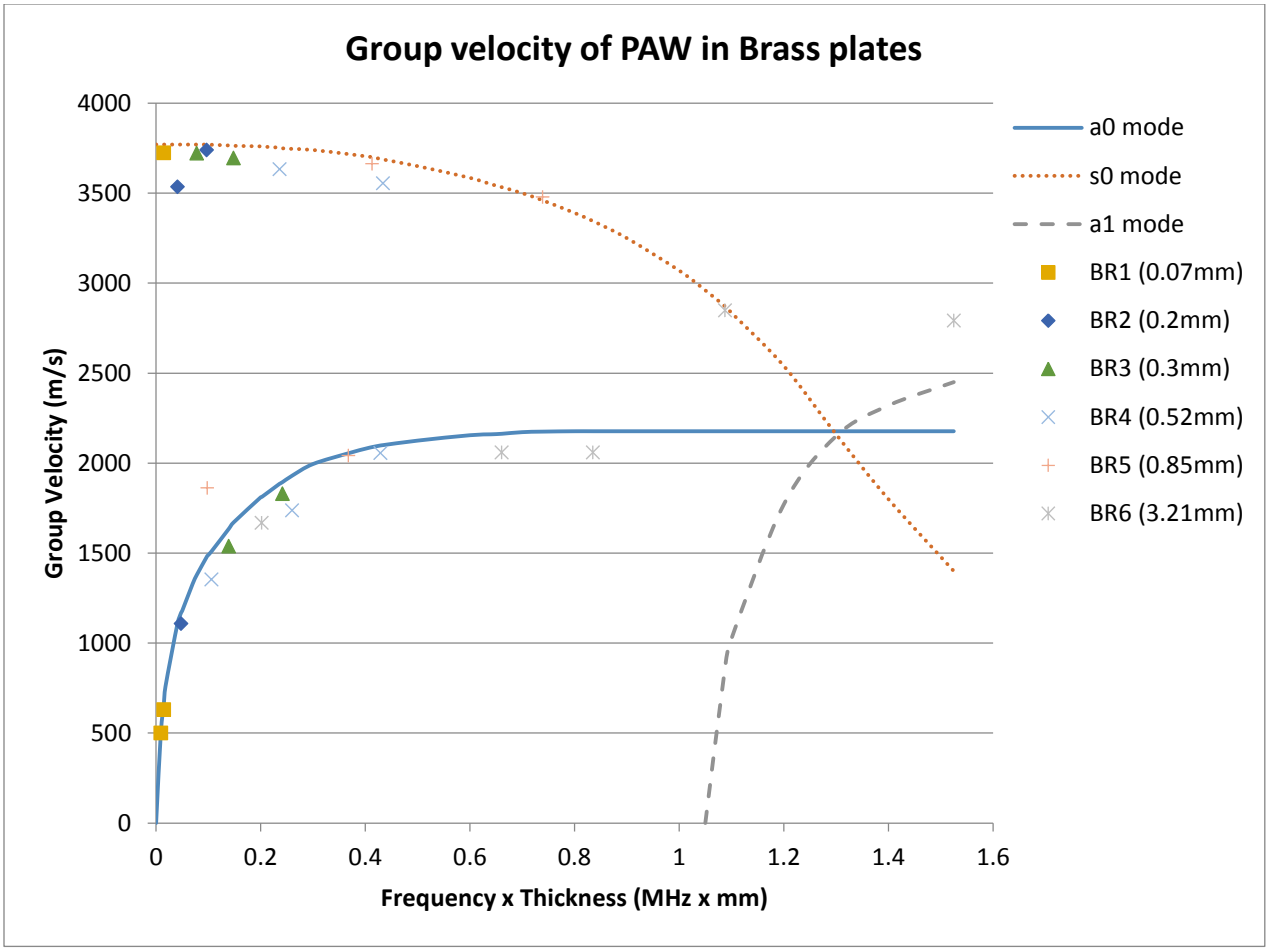

Fig. 3.19: Experimental results of group velocities of Lamb wave modes propagating through brass plates of various thicknesses at different frequencies

3.10 Group velocity of PAW in aluminium samples

Aluminium was tested with four different samples having different thicknesses. These plates had an average measured density of 2700.9 kg/m^3 which closely matched with the metal type 'Aluminium 5052' which had a density of 2690 kg/m^3 (avlandesign.com). Below are some of the oscillograms from the measurements made with aluminium plates. Only the s_0 and a_0

modes were measured as shown in figures 3.20 to 3.25 and the results for the delay are shown in tables 3.7 and 3.8.

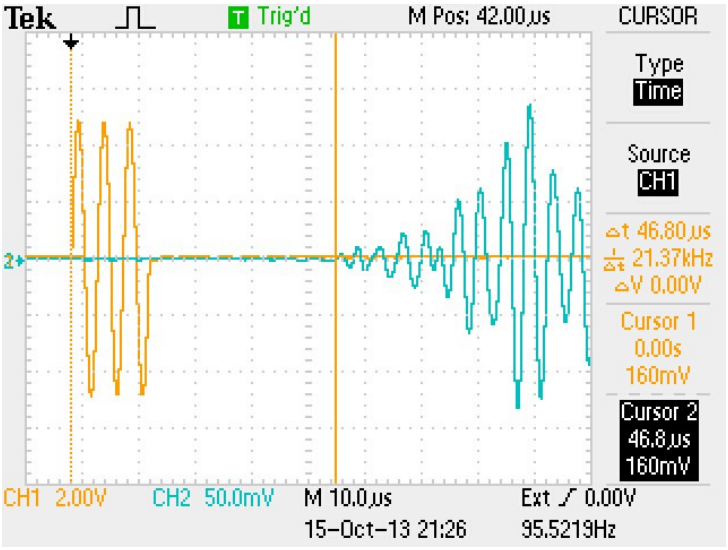

Fig. 3.20: Oscillogram containing the first few acoustic modes (green) propagated through an aluminium plate 1.55mm thick and also the input pulse (yellow) containing three cycles at a frequency of 218kHz. The yellow cursors show the measurement of delay of the a_0 mode

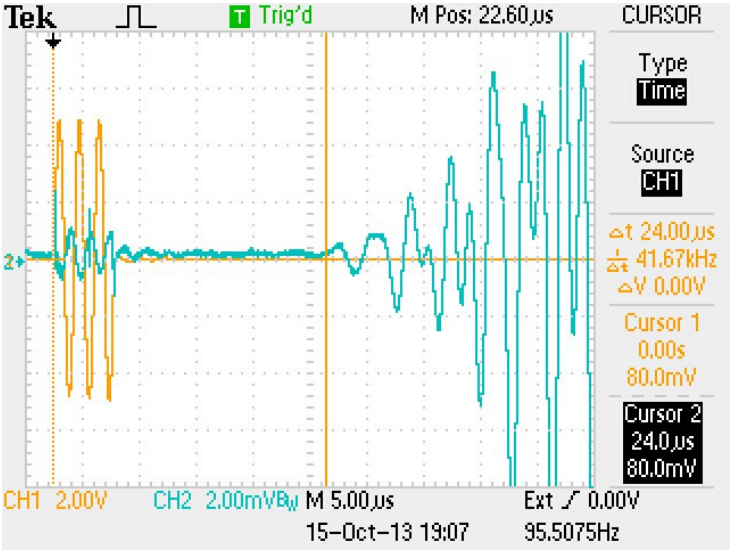

Fig. 3.21: Oscillogram showing the measurement of delay of the s_0 mode propagated through an aluminium plate 3.07mm thick at a frequency of 573kHz

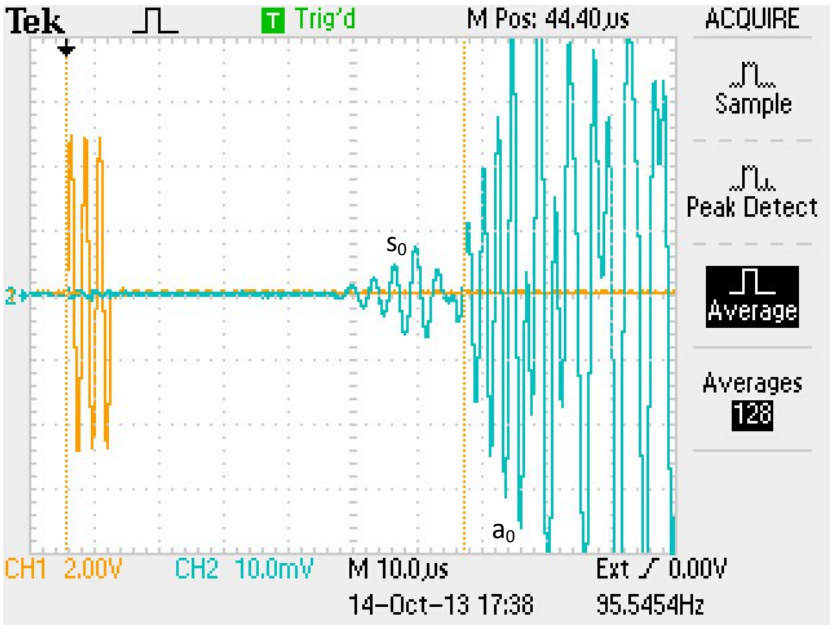

Fig. 3.22: Oscillogram showing the measurement of delay of the a_0 mode propagated through an aluminium plate 4.67mm thick at a frequency of 447kHz

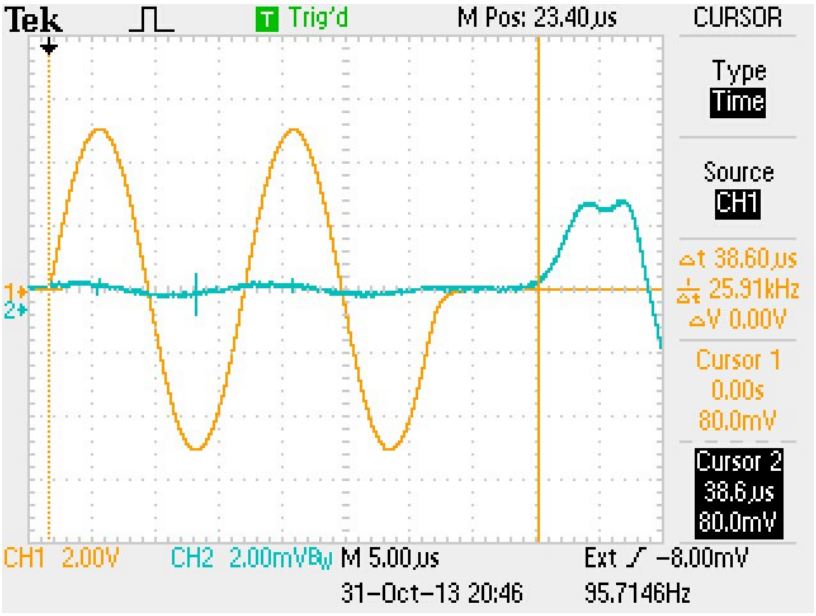

Fig. 3.23: Oscillogram showing the measurement of delay of the s_0 mode propagated through an aluminium plate 4.67mm thick at a frequency of 66kHz

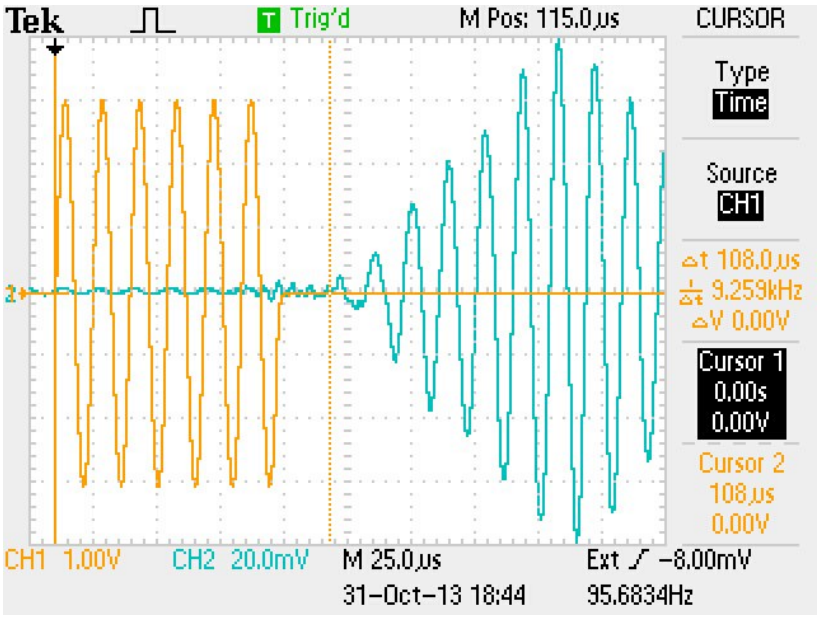

Fig. 3.24: Oscillogram showing the measurement of delay of the a_0 mode propagated through an aluminium plate 2.45mm thick at a frequency of 69kHz

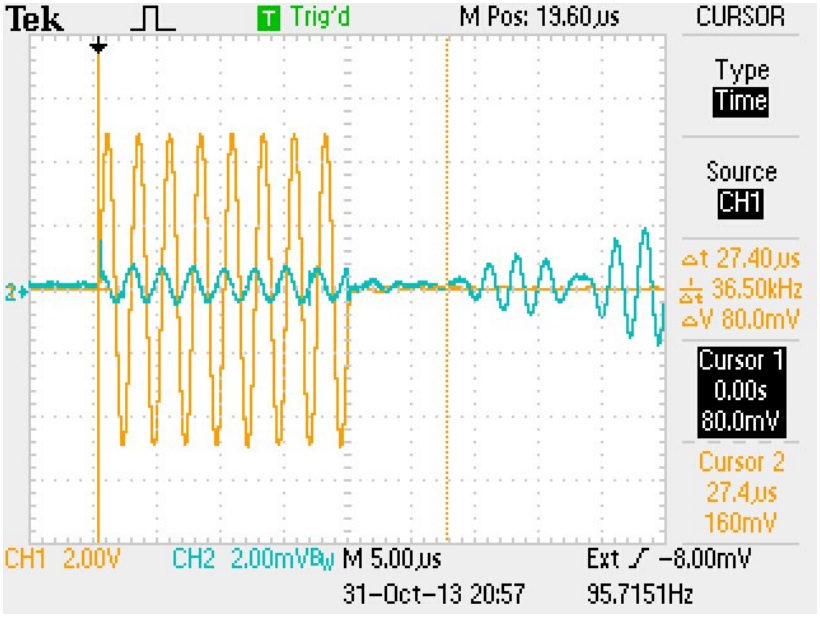

Fig. 3.25: Oscillogram showing the measurement of delay of the s_0 mode propagated through an aluminium plate 1.55mm thick at a frequency of 408kHz

Table 3.7: Measurements of delays of several propagated acoustic modes in aluminium plates of different thicknesses for a variety of frequencies

Plate Thickness (mm)	Distance between transducers (mm)	Frequency (kHz)	Delay (μs)	
			a_0	s_0
1.55	129	99	60.8	
		218	46.8	
		298	45.2	
	128	408		27.4
		1300		44.8
2.45	202	69	108	
	207.5	216	65.2	
		287		39
		465	69.6	43.2
3.07	105	133	34.8	
		296		22
		442	36.2	
		573		24
4.67	200	66		38.6
		186		40.4
		238		40
		293		40.6
	180	447	61.6	
	200	200	66	

Table 3.8: Group velocities of acoustic modes a_0 and s_0 through aluminium plates at different frequency-thickness combinations

Frequency x Thickness (MHz x mm)	Group velocity (m/s)	
	a_0	s_0
0.153	2121.71	
0.169	1870.37	
0.308		5181.35
0.338	2756.41	
0.408	3017.24	
0.462	2853.98	
0.529	3182.5	
0.632		4671.53
0.703		5320.5
0.869		4950.5
0.909		4772.73
0.934	3030.3	
1.111		5000
1.139	2981.32	4803.24
1.357	2900.55	
1.368		4926.11
1.759		4375
2.015		2879.46
2.087	2922.08	

These results are then compared with the curve below (figure 3.26) obtained from [9] and edited so that it can be compared with the results of this experiment. Notice that the a_1 mode is not shown although it exists within the frequency-thickness range considered. So the group velocities of only the s_0 and a_0 modes are measured and compared.

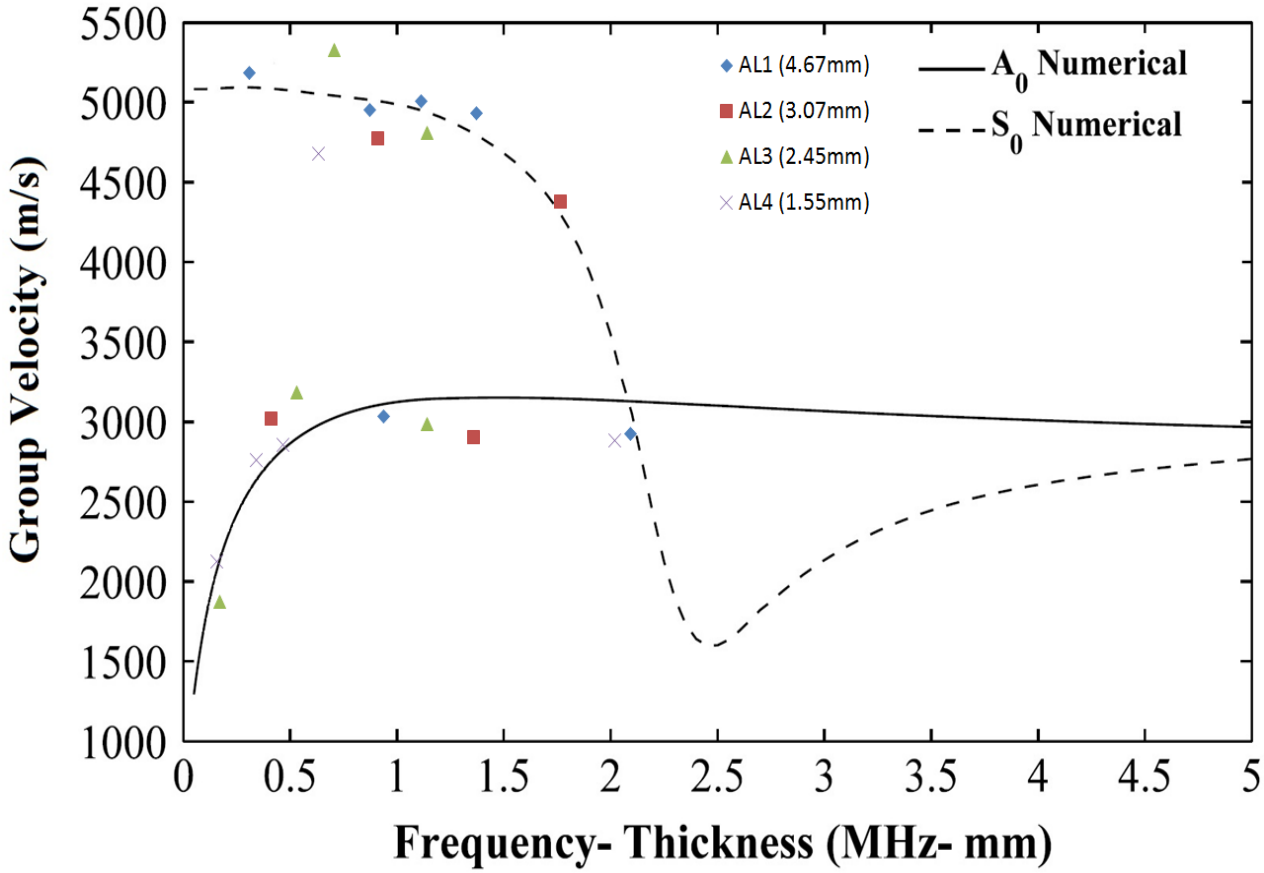

Fig. 3.26: Comparison of experimental results (points) of group velocities of Lamb wave modes propagating through aluminium plates of various thicknesses at different frequencies, with the theoretical curves (solid and dashed lines) [9]

3.11 Experimental setup for lithium niobate ($LiNbO_3$)

A single crystal of YZ-cut lithium niobate was used for the experiment. The YZ-cut means that the plate acoustic waves travel along the Z-axis in the Y-cut plate as shown in figure 3.27. Two electrodes were in contact with either end of the crystal's plate surface as shown in figure 3.28 connecting it to the function generator and the oscilloscope using wires and cables. The rest of the setup was similar to the one used with brass and aluminium with another two electrodes directly on the opposite side of the plate grounded to a metal surface which provided the base for the crystal. The crystal is excited by itself using the piezoelectric effect of lithium niobate instead of using transducers as in the previous experiments. When the electronic signal from the function generator is received, the piezoelectric crystal produces acoustic waves and vibrates accordingly.

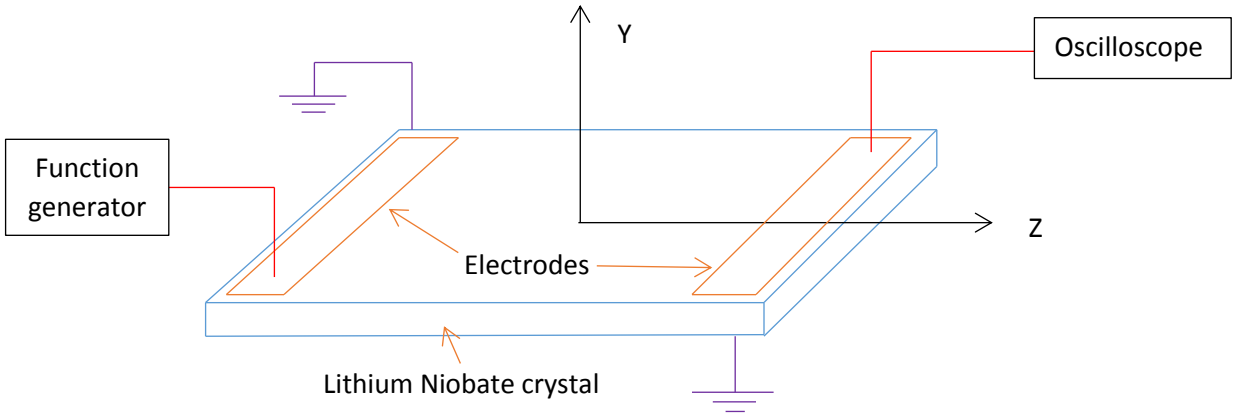

Fig. 3.27: YZ-cut of the lithium niobate crystal shown along with the experimental setup

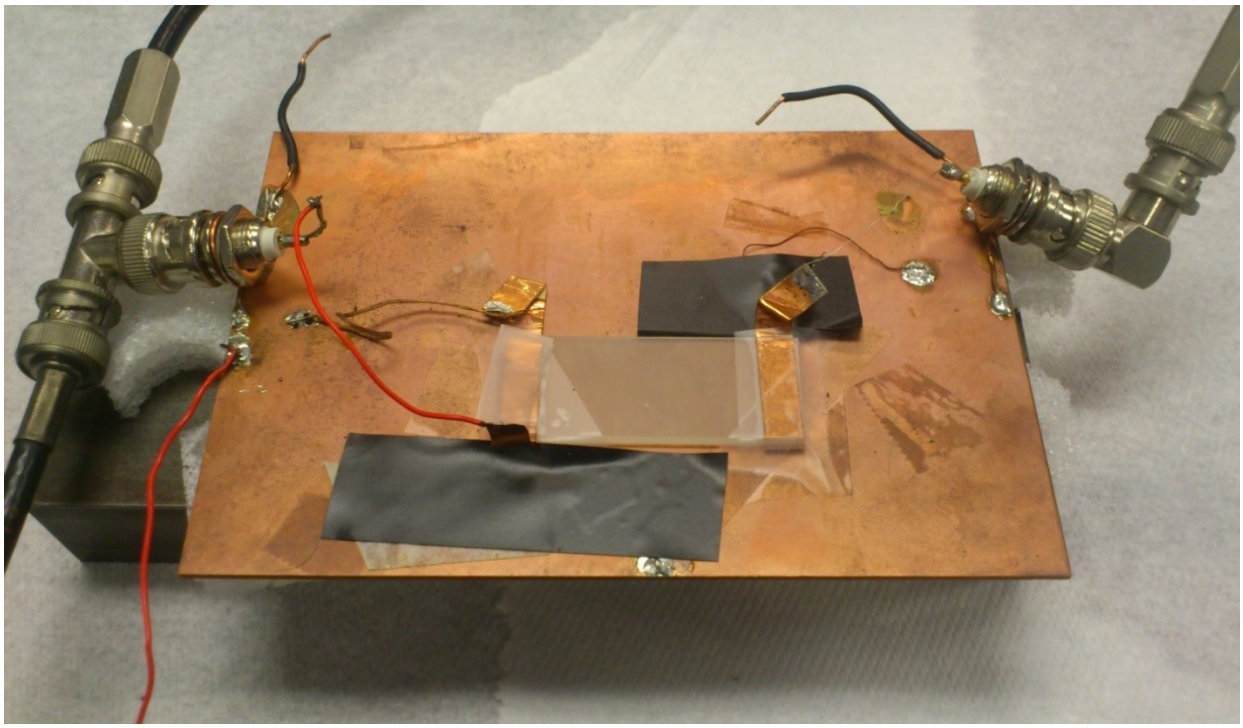

Fig. 3.28: Experimental setup used for excitation and detection of PAW through a lithium niobate plate of thickness 1.8mm

3.12 Dispersion of s_0 mode in YZ-cut lithium niobate

The experiment for lithium niobate was done using a crystal with dimensions 49mm x 19mm x 1.8mm. It was excited with frequencies ranging from as low as 153kHz up to 2.5MHz. At higher frequencies the output signal becomes weak and hard to measure. The plate gets excited at its own frequency so that the piezoelectric coupling constant is the highest, usually a sub-harmonic of the original frequency. The group velocity of the s_0 mode was calculated by obtaining the delay of the output wave for each of the frequencies. Due to the usage of only one plate and thus the thickness being constant at 1.8mm, the group velocity was plotted against frequency of the input signal. As high a number of bursts within a pulse were used in order to

minimize the scattering of frequencies of the input signal, thus the occurrence of slight overlaps of the input wave with the output waveform. Some oscillograms showing the measurement of the delay of s_o mode through lithium niobate are displayed in figures 3.29 to 3.32. The measurements from these oscillograms are recorded in table 3.9 and are then plotted in figure 3.35.

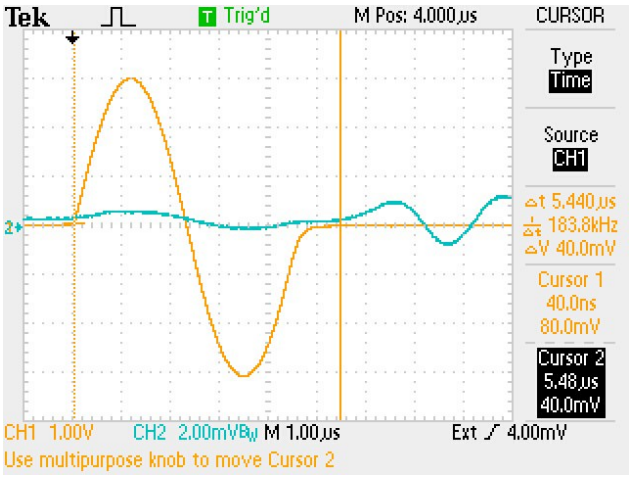

Fig. 3.29: Oscillogram containing the s_o mode (green) propagated through a lithium niobate plate 1.8mm thick and also the input pulse (yellow) containing one burst at a frequency of 215kHz. The yellow cursors show the measurement of delay of the s_o mode

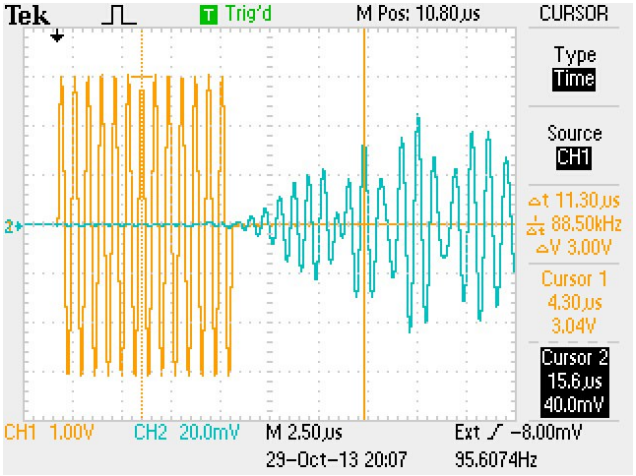

Fig. 3.30: Oscillogram showing the measurement of delay of the s_o mode at 1.5MHz

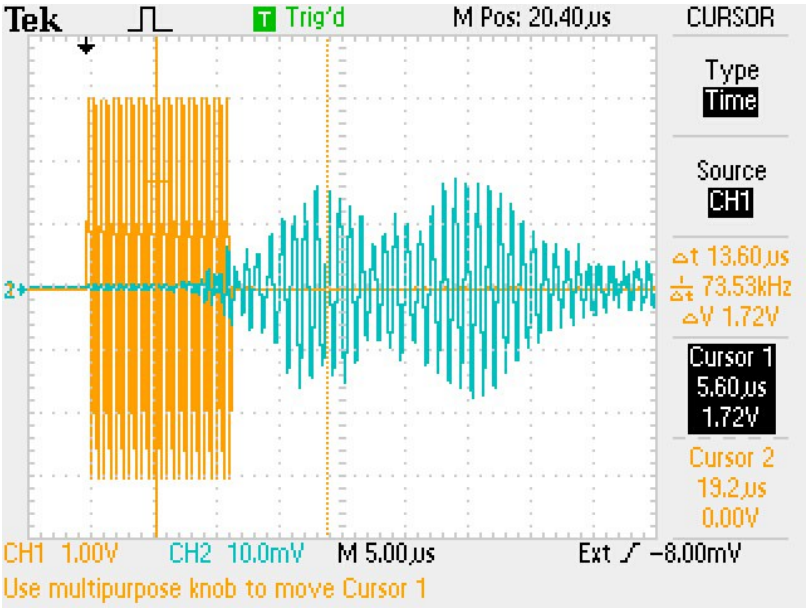

Fig. 3.31: Oscillogram showing the measurement of delay of the s_o mode at 2.04MHz

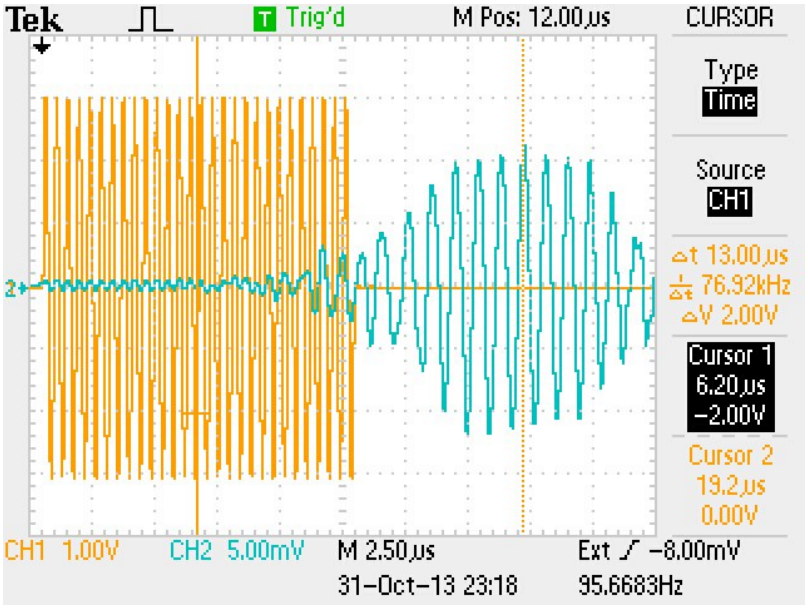

Fig. 3.32: Excitation burst and subharmonic generated at half of the excitation frequency of 2.3MHz

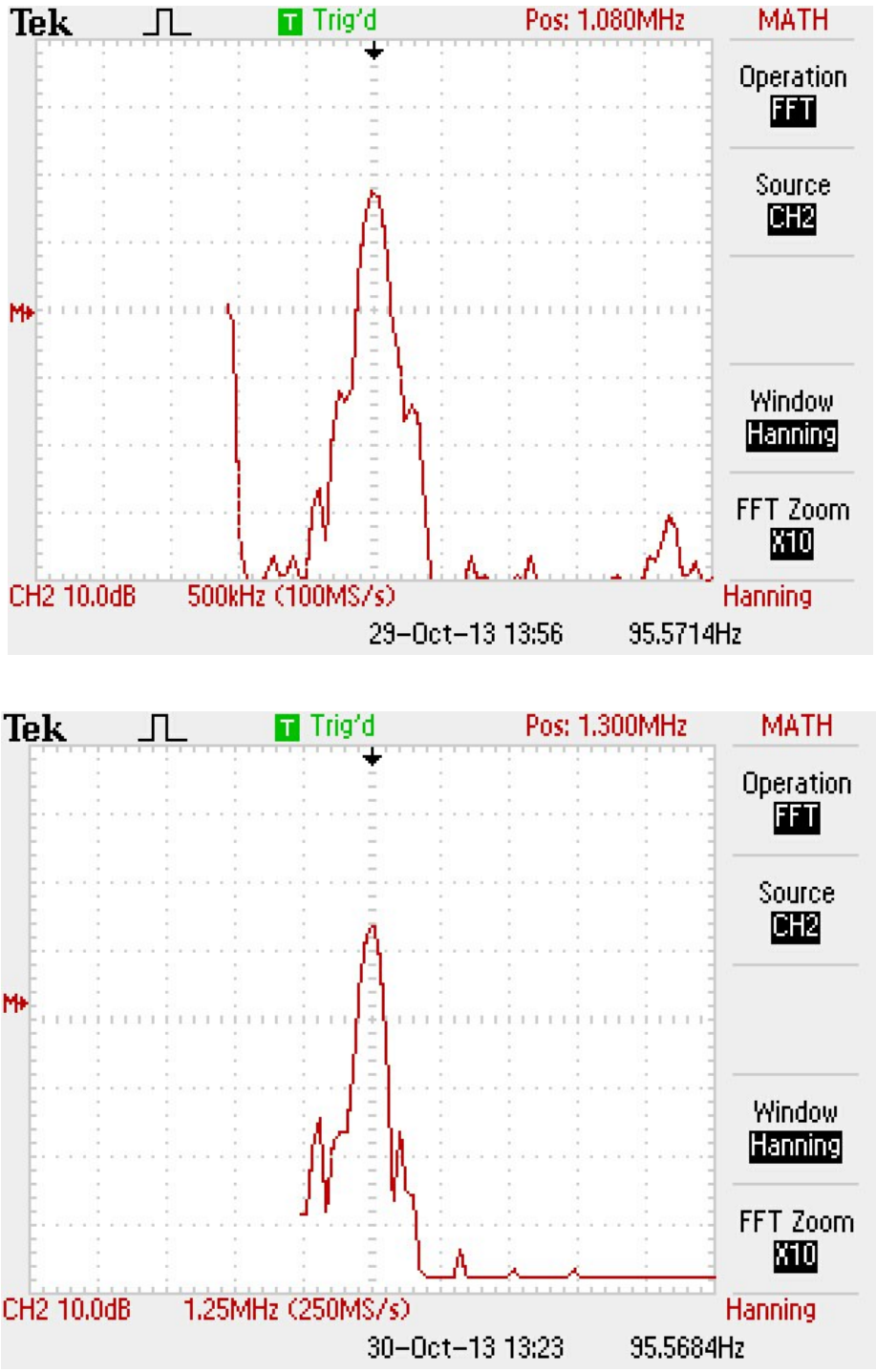

Fig. 3.33: Fast Fourier Transforms of the output waveforms of PAW in lithium niobate at excited frequencies of 1.13MHz (top) and 1.3MHz (bottom)

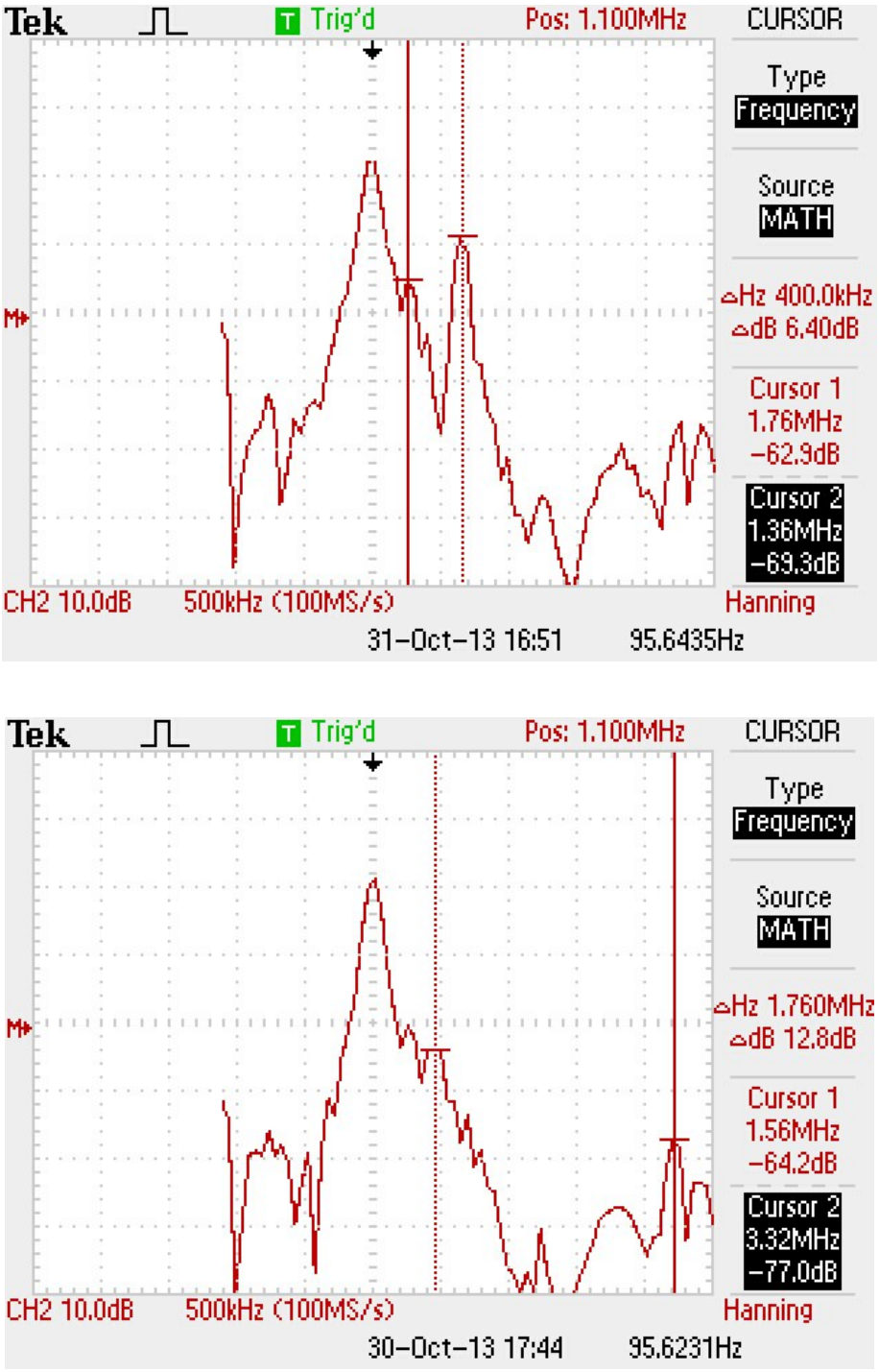

Fig. 3.34: Fast Fourier Transforms of the output waveforms of PAW in lithium niobate at excited frequencies of 1.59MHz (top) and 1.65MHz (bottom) showing the measurements of detected frequency peaks with cursors

Table 3.9: Measurements of the s_0 mode through the $LiNbO_3$ plate at a variety of frequencies

Main frequency (MHz)	Detected frequency of excited s_o mode (MHz)	Delay (μs)	Group Velocity (m/s)
0.153	0.5263	5.40	6851.85
0.215	0.4717	5.44	6801.47
0.345	0.4717	5.44	6801.47
0.516	0.5208	5.48	6751.82
0.676	0.6579	5.68	6514.08
0.913	0.7143	5.80	6379.31
1.13	0.6945	5.96	6208.05
1.23	1.316	6.72	5505.95
1.30	1.316	7.48	4946.52
1.40	1.351	8.96	4129.46
1.50	1.250	11.3	3274.34
1.59	1.250	16.8	2202.38
1.70	1.190	18.6	1989.25
1.78	1.190	18.0	2055.56
1.90	1.136	16.0	2312.50
2.00	1.111	13.5	2740.74
2.04	1.087	13.6	2720.59
2.30	1.111	13	2846.15
2.50	1.111	13	2846.15

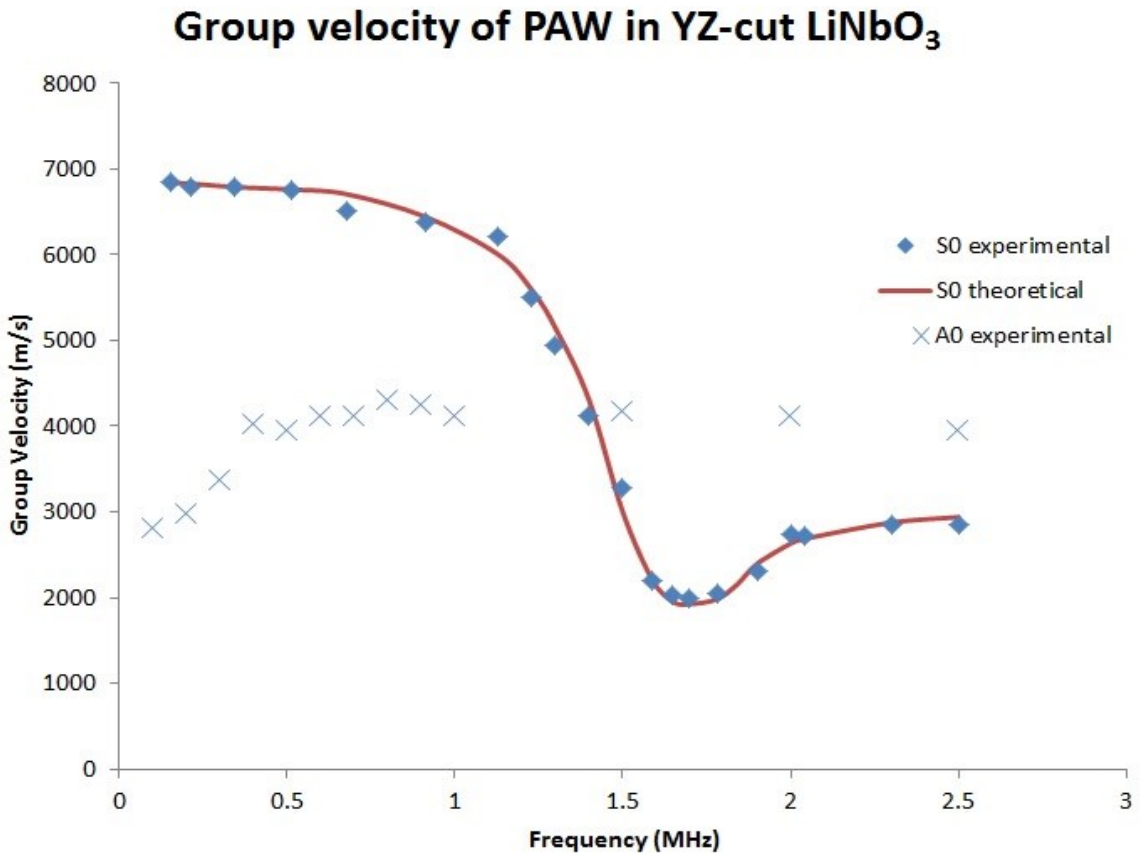

Fig. 3.35: Experimental results of the group velocity of a_o and s_o modes propagating through a YZ-cut lithium niobate plate of thickness 1.8mm, plotted against the frequency alongside the theoretical curve

3.13 Non-destructive testing (NDT)

Non-destructive testing, also known as non-destructive evaluation (NDE) is a technique used in laboratory and industry to analyze materials and their properties without causing damage to the sample examined. Importance is that the article inspected is not altered, saving time and money in the process. Application of NDT here is by propagating plate acoustic waves

through materials to be evaluated and observing the behaviour of the output. This causes no harm to the physical characteristics of the material and at the same time if a defect such as a crack, hole or a non-uniformity is present it may possibly be detected. Especially if the flaw is internal and cannot be detected with the naked eye, the only way to detect is by testing it non-destructively and in our case by propagating acoustic waves.

A primary experiment carried out in order to simply measure the thickness of a solid element or distance between given points, was the inspection of the reflected wave from an edge or discontinuity. The general method and set up are as shown below in figure 3.36. In this instance by measuring the delay of the reflected wave, the distance to the edge or discontinuity can be calculated thus giving rise to the useful application of ultrasonic thickness and distance measurements. In this process the group velocities of the fastest mode obtained in the preceding sections for different materials at different frequencies and thicknesses are made good use of.

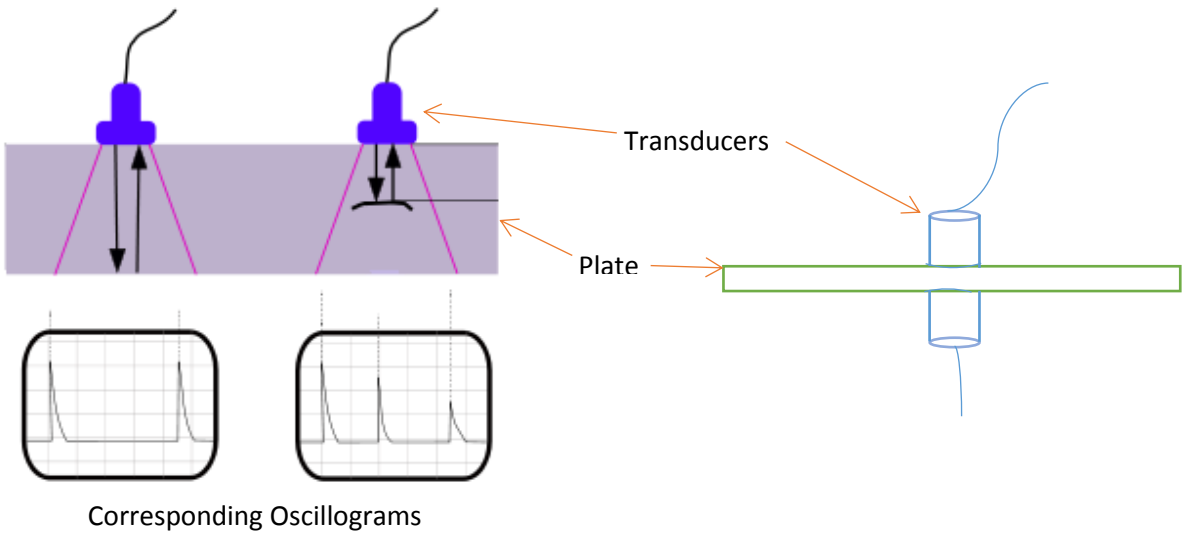

Fig. 3.36: Left: Set up showing a transducer sending acoustic waves across the thickness of a plate along with the corresponding oscillograms of the reflected waves detected, below; Right: Two transducers used, one to supply the input bursts and the other to detect the output

For this experiment an aluminium plate with thickness 2.45mm (AL3-S) was used. A circular hole with a diameter of 3mm was drilled towards the center of the plate's main surface which was 229mm in length and 94mm in width. Transducers with diameter 0.9mm each were placed on either side of the plate exactly aligning each other as shown on the right in figure 3.36 nearer to the hole than any of the edges. Two separate transducers were used, one to supply and the other to detect acoustic waves because the amplitude of the reflected wave is much lower compared to the original input signal. In order to be able to observe the reflected signal the sensitivity of the second transducer oscilloscope reading must be contrastingly higher than the first one. Usage of two different channels in the oscilloscope allows two different scales of amplitude to be used making the weaker signal visible alongside the input. Just as in the previous experiments, short bursts of ultrasonic pulses were used with center frequencies ranging from the kilohertz region up to about 5MHz. Only the first edge or discontinuity may be able to be clearly identified due to the overlaps of several signals after the occurrence of the first reflection. These may be the secondary modes of the first reflected wave and the signals coming from the eventual reflections after the first one. In the case of a discontinuity this method becomes less efficient since only a part of the wave is reflected from a crack, hole or any other kind of discontinuity, resulting in an output signal barely noticeable. Although the transducers were placed nearer to the hole than the edges, the first reflected signal detected in the output was determined to be from an edge rather than from the hole. So this method wasn't very effective in detecting defects, rather more useful in determining distances to edges or discontinuities we already knew that existed or primarily to measure thickness.

A similar but more effective method to detect defects was to send acoustic waves through a defective material plate and inspect the FFT of the output. The oscillograms of the

outputs show a slight drop in amplitude compared to the input whenever a defect was present but not to an extent to say for sure that there is a defect. Observations of the FFTs were done for the outputs from the following general experimental set up.

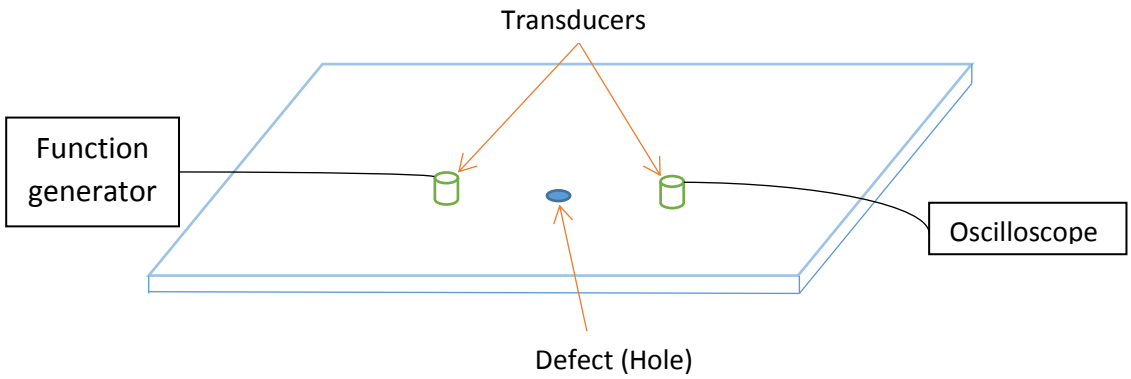

Fig. 3.37: The experimental set up used for non-destructive testing

A brass plate with thickness 0.52mm (BR4-S) was used with a 6mm diameter circular hole was drilled at the center of the plate's surface. The dimensions of the plate surface were 280mm x 152mm. Firstly the two transducers were positioned 5.7cm apart, somewhat away from the hole as shown in figure 3.38.

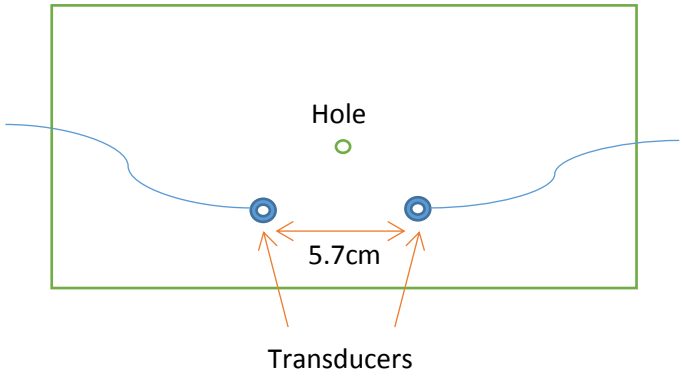

Fig. 3.38: Top view of the brass plate showing positions of the transducers with respect to the 6mm diameter hole

An acoustic signal of 50 bursts of amplitude 10V at a frequency of 4.72MHz was supplied through the input transducer. Higher frequencies were used due to the relatively small size of the hole. The output was detected through the second transducer from which the oscillogram and FFT data as shown in figure 3.40 were obtained. Then this was compared to data from another position of the transducers as shown in figure 3.39 below. The distance between the transducers were kept the same while on this occasion the acoustic waves had to travel on a path where the hole was in the way. Same acoustic signal input was provided and the oscillogram and the FFT were obtained by the oscilloscope and are shown in figure 3.40 in comparison to how they looked like earlier.

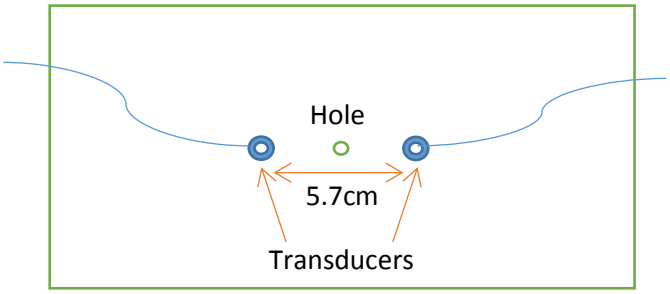

Fig. 3.39: Top view of the brass plate with the two transducers exactly aligned with the same hole in a straight line

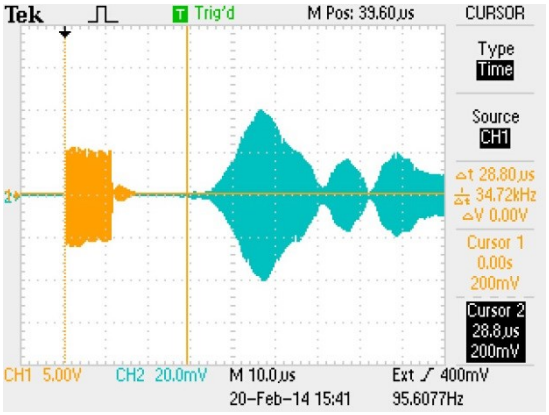

(a)

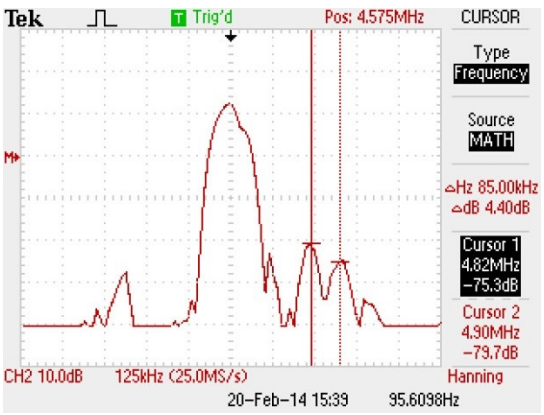

(b)

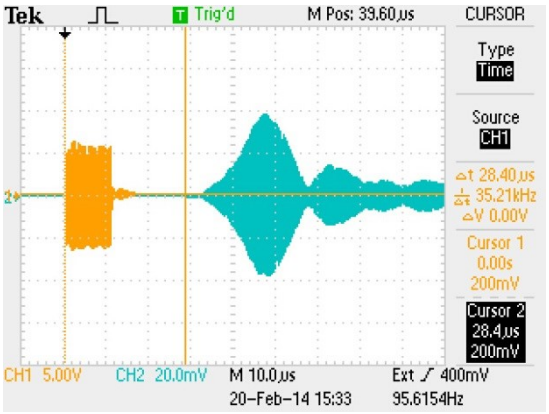

(c)

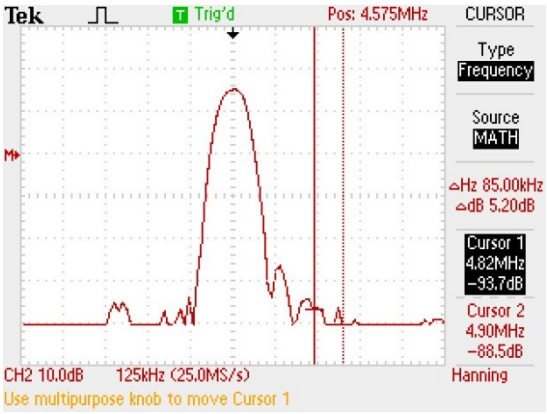

(d)

Fig. 3.40: Oscillograms ((a) and (c)) and FFTs ((b) and (d)) of the two different positionings of the two transducers in relation to the hole in the brass plate, when both are away from the hole ((a) and (b)) and when they are aligned with the hole in a straight line ((c) and (d))

As seen from the oscillograms of figure 3.40 (a) and (c), the amplitude of the whole waveform dropped slightly when the hole came in between the transducers. This does not give much of an indication that a defect is present or it may be due to the type of defect, which in this case is a circular hole. The clear contrast lies in the FFTs of the two scenarios. As seen on the

figure 3.40 (b) and (d), the side lobes of the spectra have almost completely disappeared from (b) to (d) but the main frequency at the center remains intact. In figure 3.40 (b), peaks at 4.82MHz and 4.90MHz have intensities in the order of 30dB below the center maximum at 4.575MHz whereas in figure 3.40 (d) they have dropped in intensity significantly to about 43 – 50dB below the central peak. In most cases the intensity drop is more than 10dB which is considerably high. This indicates that the frequencies that were present in that part of the spectrum have been absorbed when propagating across the hole. These absent frequencies may mean that the modes with those frequencies do not propagate across the hole. This may depend on the size and shape of the hole or defect and also on the input frequency supplied. The lower frequencies have a lesser effect since the wavelength of the acoustic waves then, is comparable to the diameter of the hole. As seen here the difference in the FFT spectra when a hole is present, can be used to detect defects and analyze them.

CHAPTER 4

CONCLUSIONS

1) The Group velocity of plate acoustic waves in four electronic materials was tested for different frequencies and thicknesses. The plots obtained from these were compared with theoretical curves contained in published work. It can be concluded that the experimental results match closely with those. So the results obtained for particular plate thicknesses and frequencies can be put to use in applications such as non-destructive testing.
2) The glass, brass and aluminium materials used here may not have been examined before since the densities of those plates used didn't exactly match with the samples used in referred previous work. So the results obtained here could be useful for future work with materials having same densities. This may also explain the slight drift away from the theoretical plots used for comparison, as these published curves were of materials with densities similar but not exact. Also some of the various thicknesses used here may not have been investigated before although they are plotted as the frequency x thickness. So the group velocity values of the particular plate used at particular frequencies can be useful in future references.
3) The four electronic materials used turned out to have similarly dispersive curves to each other, with the s_0 mode having a high dispersion at or around 1MHz-mm whereas the a_0 mode has a high dispersion at frequencies x thickness values below 500kHz-mm. As the frequency was increased from a minimum, the a_0 mode always started slower than the s_0 mode and became faster and overtook the usually decelerating s_0 mode at or around

2MHz-mm. For brass plates though, the value of the frequency thickness product in both these cases was slightly lower than the above mentioned values.

4) In the glass plate examined, the group velocity of the a_0 mode increased rapidly from zero to a maximum of about 3200m/s in the low frequency x thickness region until about 900kHz-mm then remained approximately constant for higher frequency x thickness values thereafter. The s_0 mode started from around 5400m/s and decreased rapidly between 1MHz-mm and about 2.5MHz-mm to a minimum of about 1600m/s and increased again to about 2900m/s. This was consistent with the usual dispersion observed in the s_0 mode.
5) In the six brass plates tested, it is found that the highest velocity of a mode is about 3750m/s, which is of the s_0 mode at very low frequencies. This decreased as the frequency x thickness was increased and dipped below the a_0 and the a_1 mode at about 1.25MHz-mm. The group velocity of the a_0 mode increased rapidly from zero to about 2200m/s until the frequency thickness product reached a value of about 0.5MHz-mm and thereafter remained constant throughout. An experimental point was obtained for the a_1 mode as well which happened to be slightly faster than it should theoretically have been, none the less the existence of the a_1 mode was confirmed. As seen in figure 4.18 there exists a frequency x thickness value in which the group velocities of all three modes s_0, a_0 and a_1 are equal, a fact which could be useful in applications.
6) In the four aluminum plates examined, it is found that the highest group velocity is around 5200m/s in the s_0 mode at frequencies below about 1MHz. This decreased gradually till about 1.5MHz-mm and then rapidly from there on till about 2.5MHz-mm and increased again thereafter. As usual, the group velocity of the a_0 mode starts at 0m/s

and increases rapidly to about 3000m/s in the region below 1MHz-mm and then remains approximately constant throughout overtaking the s_0 mode at around 2.1MHz-mm. Aluminum is used vastly in the aviation industry and is frequently investigated for cracks within the metal. Since a crack is similar to a hole with a lesser diameter to the one experimented in the work, an existence of a crack would mean that experimental curves of it would drift away significantly from the ones obtained here. So this experimental analysis can be extremely useful in the industry.

7) The group velocity of acoustic waves through a YZ-cut lithium niobate plate was investigated for the first time. The plot of the s_0 mode through YZ-cut lithium niobate was found to be consistent with the usual dispersion seen of an s_0 mode. It is found that at very low frequencies the s_0 mode has its highest group velocity of about 7000m/s, which is significantly higher than the other three materials investigated. This velocity decreases gradually in the frequency region below 1.2MHz and then rapidly from there on till about 1.6MHz. It reaches a minimum of about 2000m/s at 1.7MHz and thereafter increases again between frequencies 1.7MHz and 2MHz and remains approximately constant there onwards. This analysis could be very useful for future work in the field as YZ-cut lithium niobate has many applications but rarely has been investigated for the group velocity of PAWs in them. Future work can be built on this analysis by the measurement of the group velocity of the a_0 mode and some higher order modes as well.
8) By the inspection of the Fast Fourier transforms of the inputs and outputs, the existing frequencies in the waveform can be determined. It is seen that the most abundant frequencies of the waveform are shown as peaks in the FFT. It is found that the FFT of the input has a clear peak at the main frequency provided by the function generator when

a higher number of bursts of were applied while a scattered frequency spectrum is observed around that central frequency when a lower number of bursts were applied. There is usually more than one peak in output FFT oscillograms meaning that the plate is excited in more than one frequency. Sometimes in $LiNbO_3$ a sub-harmaonic acoustic mode is excited as well. It can be explained by a frequency dependent electromechanical coupling factor in a lithium niobate plate. Thus separate modes can be identified with the help of FFTs. It can be concluded that the FFT function is very useful in analyzing oscillograms.

9) A very useful application of plate acoustic waves is thickness or distance measurements. Using the experimental results obtained regarding group velocities of PAW in the four electronic materials examined, thickness or distance measurements for same material plates were able to be done. This involved studying and measurement of the reflected signal from an edge or discontinuity. It is found that the calculations of distances to edges were fairly accurate although it wasn't the case regarding less sharp discontinuities due to the fact that the wave is only partially reflected. So this method wasn't that effective in detecting discontinuities but rather to simply calculate distances to ones already known.
10) Detecting defects or discontinuities was also experimented. This time the wave propagated rather than the wave reflected was considered. Examination of FFTs rather than oscillogram data of the propagated output, proved more likely to yield information about existing discontinuities. It was seen that the amplitude of the whole output waveform drops when a defect is encountered. This observation alone couldn't be used as an identification of a defect since the drop was usually very small. Instead FFTs revealed that the intensities of several frequencies besides the center frequency dropped

significantly when encountered with a discontinuity. This meant that those frequencies were absorbed by the hole or in other words, they were not able to propagate across it. So several modes with those frequencies were almost completely blocked off. It can be concluded that this phenomenon could be used to detect certain types of defects and the FFTs help immensely in the process.

REFERENCES

[1] J. David N. Cheeke; Fundamentals and applications of ultrasonic waves; 1st edition; CRC press (2002)

[2] Warren P. Mason; Physical Acoustics: Principles and Methods; Volume I - Part A; Academic press (1964)

[3] Gordon S. Kino; Acoustic waves: Devices, imaging and analog signal processing; Prentice-Hall, inc. (1987)

[4] Victor Klymko, Andriy Nadtochiy and Igor Ostrovskii; Theoretical and experimental study of plate acoustic waves in ZX cut Lithium Niobate; IEEE Transactions on Ultrasonics, Ferroelectrics, and Frequency Control, vol. 55, no. 12, December 2008

[5] Sourav Banerjee, Tribikram Kundu; Ultrasonic field modeling in plates immersed in fluid; International Journal of Solids and Structures 44 (2007) 6013–6029; February 2007

[6] Daniel Royer, Eugene Dieulesaint; Elastic waves in solids II: Generation, Acousto-optic interaction, Applications; Springer (1999)

[7] A. W. Warner, M. Onoe and G. A. Coquin; Determination of Elastic and Piezoelectric Constants for Crystals in Class (3m); The Journal of the Acoustical Society of America, Volume 42, Number 6, 1967, Page 1223

[8] Wei-Hua Wang, R. J. Wang, F. Y. Li, D. Q. Zhao, and M. X. Pan; Elastic constants and their pressure dependence of $Zr_{41}Ti_{14}Cu_{12.5}Ni_9Be_{22.5}C_1$ bulk metallic glass; Applied Physics letters, Volume 74, Number 13, 29 March 1999

[9] B Poddar, A Kumar, M Mitral and P M Mujumdar; Time reversibility of a Lamb wave for damage detection in a metallic plate; Smart materials and structures, 6 January 2011

[10] P. Fromme, P. Cawley, P. Wilcox; Development of a Permanently Attached Guided Wave Array for the Monitoring of Structural Integrity; NDT.net, Vol. 9 No.02, February 2004

[11] Eric L. Adler; Electromechanical Coupling to Lamb and Shear-Horizontal Modes in Piezoelectric Plates; IEEE Transactions on Ultrasonics, Ferroelectrics and Frequency Control, Vol. 36. No. 2. March 1989

[12] Waldemar Soluch and Magdalena Lysakowska; Properties of Acoustic Plate Modes in YZ LiNbO3; IEEE Transactions on Ultrasonics, Ferroelectrics, and Frequency Control, vol. 60, no. 1, January 2013

[13] I.E. Kuznetsova, B.D. Zaitsev, I.A. Borodina, A.A. Teplyh, V.V. Shurygin, S.G. Joshi; Investigation of acoustic waves of higher order propagating in plates of lithium niobate; Ultrasonics 42 (2004) 179–182

[14] Peter Huthwaite, Francesco Simonetti; High-resolution guided wave tomography; Wave Motion 50 (2013) 979–993

APPENDICES

APPENDIX A: SOLID - SOLID INTERFACE

There are two reflected and two transmitted waves for an incident longitudinal (P) or bulk shear wave (SV).

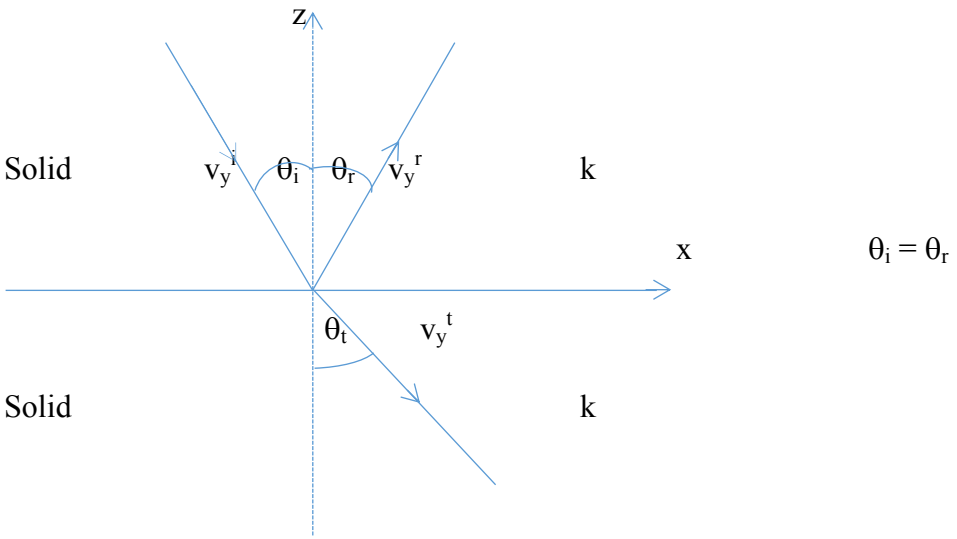

Fig. A.1: Reflection and transmission of acoustic waves at a solid-solid interface

There is no coupling between SH modes and P and SV waves. For SH modes, the particle velocities (v_y) can be written as [1],

$$v_y^i = A \exp j(\omega t - k \, sin\theta_i x + k \cos \theta_i z) \quad \text{(A.1)}$$

$$v_y^r = B \exp j(\omega t - k \, sin\theta_i x - k \cos \theta_i z) \quad \text{(A.2)}$$

$$v_y^t = C \exp j(\omega t - k \sin \theta_i x + k \cos \theta_t z) \quad \text{(A.3)}$$

Where A, B and C are constants.

Then the normal and tangential stresses are [1],

$$T_{yx} = \frac{c_{44}}{j\omega} \left(\frac{\partial v_y}{\partial x} \right) \quad \text{(A.4)}$$

$$T_{yz} = \frac{c_{44}}{j\omega}\left(\frac{\partial v_y}{\partial z}\right) \quad \text{(A.5)}$$

At a free boundary an SH wave is reflected and converted in to another SH wave with no mode conversion. For SV and P waves reflection coefficients can be calculated using boundary conditions of zero normal and tangential stress at the boundary. If L stands for longitudinal waves and S stands for shear waves, they are related as,

$$R_{LL} = -R_{SS} \quad \text{(A.6)}$$

$$R_{LL}^2 + R_{LS}\, R_{SL} = 1 \quad \text{(A.7)}$$

APPENDIX B: CRYSTAL ACOUSTICS

By using the strain tensor, the equation of motion of a wave propagating in the x direction can be written as [1],

$$\rho \frac{\partial^2 u_i}{\partial t^2} = c_{ijkl} \frac{\partial^2 u_l}{\partial x_j \partial x_k} \tag{B.1}$$

A wave in a bulk medium in three dimensions can be written in the form,

$$u_l = u_{0l} \exp j(\omega t - \vec{k}.\vec{r}) \tag{B.2}$$

where,

ω – angular frequency

k – propagation vector

For bulk waves propagating in isotropic media there is one longitudinal mode and two transverse modes. For crystalline media three independent waves may be propagated with each having a particular phase velocity and the displacements are perpendicular to each other. These are neither longitudinal nor transverse. However depending on the crystal structure there are certain directions which pure waves can be propagated in.

From (B.1) and (B.2) Christoffel's equation can be obtained as,

$$\rho V_p^2 u_{0i} = c_{ijkl} n_k n_j u_{0l} \tag{B.3}$$

where,

n – propagation direction

B.1 Group velocity and characteristic surfaces

The crystal structure imposes restrictions on the allowed directions of propagation of pure modes and also energy, which may be different from the propagation of the wave. By using the acoustic Poynting's vector, the relation between the energy propagation velocity and phase velocity can be expresses as,

$$V_{ei} = \frac{c_{ijkl} u_{0j} u_{0l} n_k}{\rho V_p} \tag{B.4}$$

where,

V_e = energy propagation velocity

This implies that the projection of the energy propagation velocity on the propagation direction yields the phase velocity. In linear acoustics the energy propagation velocity is equal to the group velocity (V_G) and can be expressed as,

$$V_{Gj} = \frac{\partial V_p}{\partial n_j} \tag{B.5}$$

The direction of the group velocity is perpendicular to a constant energy surface in k-space as seen in figure B.1 below. Acoustic wave propagation in anisotropic solids can be described by constructing several different surfaces. For every case there are three shells, one quasi-longitudinal and two quasi-shear.

As shown below, the velocity surface traces out the phase velocity as a function of direction. The slowness surface shows the variation of $1/V_P$ in k/ω space. It is a surface of constant ω. For a point on the surface, the radius vector gives $1/V_P$ for that direction and the group velocity is normal to the slowness surface. Then the wave surface is the locus of the group

velocity as a function of direction. It gives the distance traveled by a wave emitted from the origin within a certain time. This time is fixed due to it being an equiphase surface. For a given point on the surface the propagation vector for a plane wave is perpendicular to the surface.

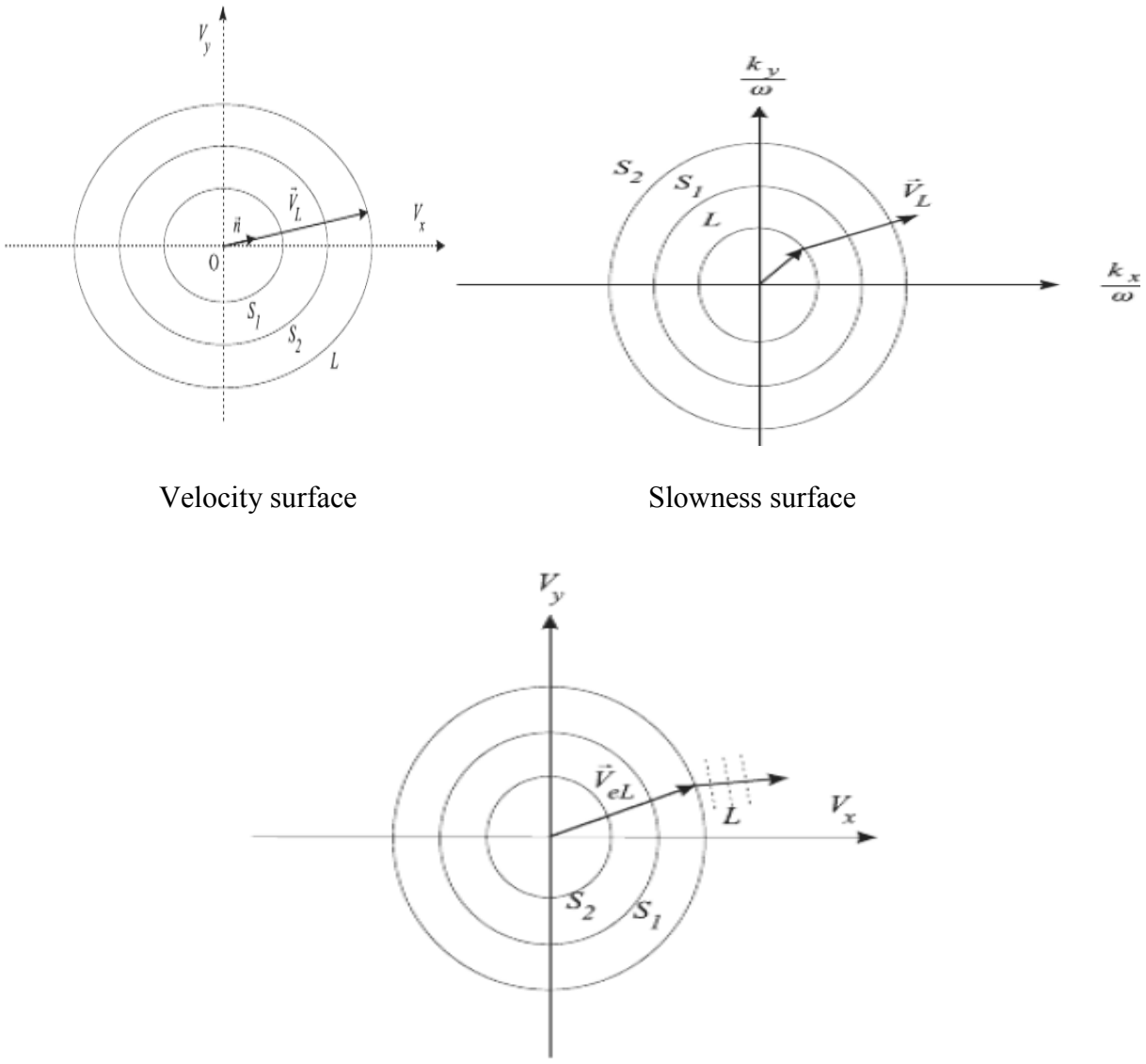

Velocity surface

Slowness surface

Wave surface

Fig. B.1: Characteristic surfaces for acoustic wave propagation in anisotropic solids [1]

APPENDIX C: PIEZOELECTRIC MATERIALS AND APPLICATIONS

C.1 Piezoelectricity

Piezoelectricity is the electric charge internally generated in a solid in response to an applied mechanical stress. It is actually the electromechanical interaction between the mechanical and the electrical state in crystalline materials with no inversion symmetry, i.e. not containing an inversion center as one of its symmetry elements. It is a reversible process in which in some materials, internal generation of mechanical strain occurs due to an applied electric field. Piezoelectric effect is very useful in production and detection of sound and generation of high voltages and frequencies.

A necessity for piezoelectricity to occur is the absence of a center of symmetry meaning the media are intrinsically anisotropic. Piezoelectricity involves an interaction between the elastic and dielectric phenomena and therefore dielectric and elastic constants are useful in regards to piezoelectric properties. These coefficients are usually arranged in a 9×9 matrix in which each column refers to one stress variable as the independent variable and each row to a strain variable as the dependent variable. The matrix is symmetrical so that in general there are 45 coefficients comprising 21 elastic compliances (s_{ij}^{E}), 6 permittivities (ϵ_{im}^{T}) and 18 piezoelectric constants (d_{ik}). Here E and T refer to constant electric field and constant elastic stress respectively. The dots or filled circles mean a non-zero component, blank spaces are zero coefficients, tie lines mean equality required by symmetry and open circles mean equal value but opposite sign as seen in figure C.1.

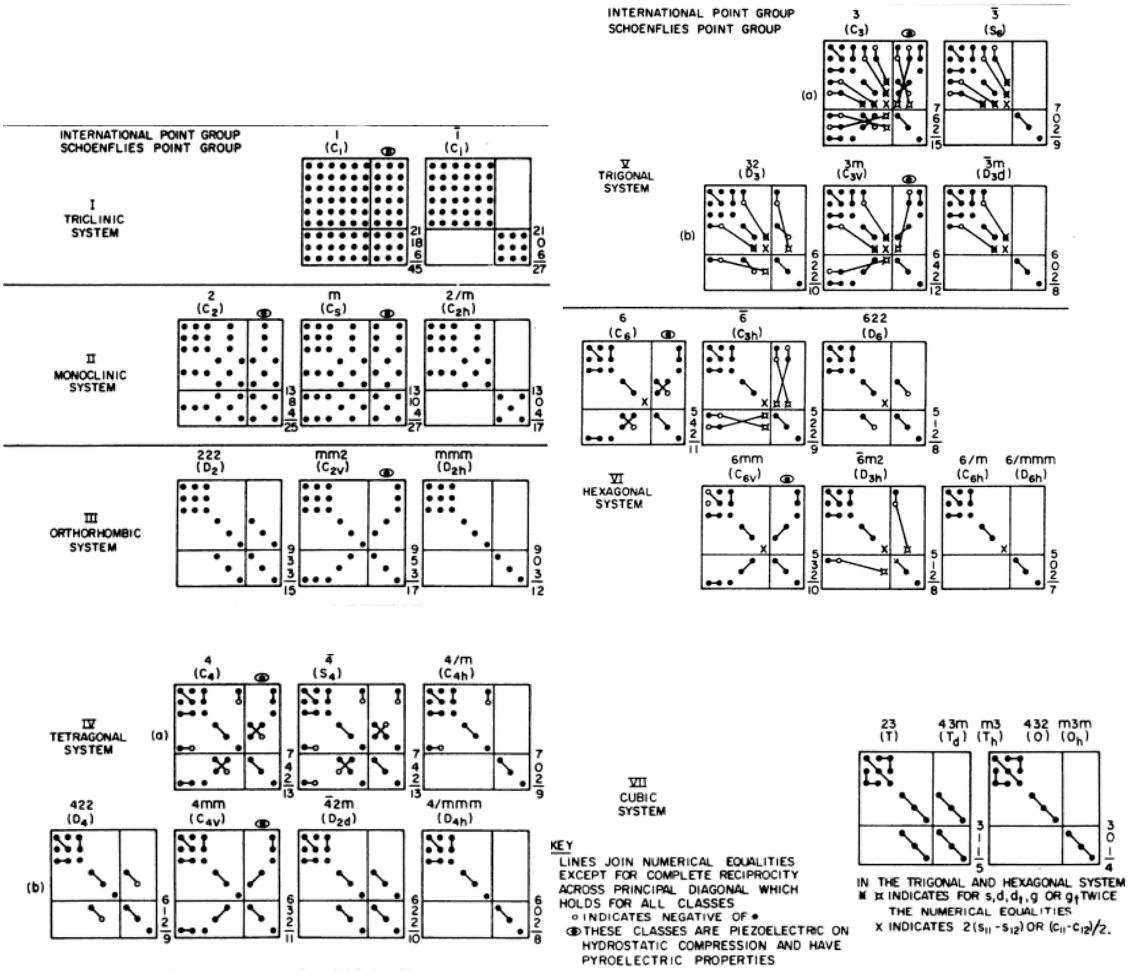

Fig. C.1: Elasto-electric matrices for the 32 crystal classes [2]

Piezoelectric crystals can be used to generate and detect ultrasonic waves since the indirect piezoelectric effect is still works at high frequencies. A necessary but not sufficient condition for piezoelectricity is the absence of a center of symmetry since the occurrence of electric dipole moments in solids is due to ions on crystal lattice sites with asymmetric charge surroundings being induced. The sign of the induced potential difference depends on whether a compression or an expansion was applied. For dielectric media, two piezoelectric constitutive relations can be written as [1],

$$D_i = \varepsilon_0 E_j + P \quad \text{(C.1)}$$

where,

D – electric displacement

E – electric field

ε_0 – permittivity

P – polarization

and,

$$T_{kl} = c_{ij}^{E} S_{ij} - e_{ijk} E_j \quad \text{(C.2)}$$

where,

e – piezoelectric stress constant

C.2 Piezoelectric coupling factor

Denoted as K^2, the electromechanical coupling coefficient is a numerical measure of conversion efficiency of electrical energy in to acoustic energy or vice versa in piezoelectric materials. It expresses the coupling of electrical and mechanical energy. This can be expressed as [2],

$$K = \frac{U_m}{\sqrt{U_e U_d}} \quad \text{(C.3)}$$

Where,

U_m = mutual energy between electrical and acoustic components

U_e = elastic energy

U_d = dielectric energy

The one dimensional equation of motion for the propagation of acoustic waves along the z-axis in a piezoelectric medium can be obtained as [1],

$$\rho \frac{\partial^2 u}{\partial t^2} = c^E \left(1 + \frac{e^2}{c^E \varepsilon^S}\right) \frac{\partial^2 u}{\partial z^2} \tag{C.4}$$

As seen from equation (C.4) the sound velocity in a piezoelectric medium V_L^D is stiffened compared to the usual sound velocity $V_L = \sqrt{\frac{c^E}{\rho}}$ as follows,

$$V_L^D = V_L \sqrt{1 + K^2} \tag{C.5}$$

where the piezoelectric coupling constant,

$$K^2 = \frac{e^2}{c^E \varepsilon^S} \tag{C.6}$$

This is valid only when D = 0 and for transversely clamped transducers where width is much greater than the wavelength. The impedance of a transducer is determined by the effective coupling constant k_T^2,

$$k_T^2 = \frac{K^2}{1 + K^2} \tag{C.7}$$

Piezoelectric coupling factor can be written as,

$$K^2 = \frac{U_{elec}}{U_{elas}} \tag{C.8}$$

where,

U_{elec} – stored electrical energy

U_{elas} – stored elastic energy

C.3 Equations of the piezoelectric medium

These equations are derived from thermodynamic potentials. The piezoelectric constants relate 2nd order symmetric tensors to vectors and they themselves are 3rd order tensors. The elastic constants relate two 2nd order symmetric tensors and are 4th order tensors themselves. The dielectric constants relate two vectors and therefore are 2nd order tensors themselves. In the most general case magnetic field should also be included, which gives [2],

$$G = U - S_i T_i - E_m D_m - H_m B_m - S\theta \qquad \text{(C.9)}$$

Where,

D – electric displacement component

H – magnetic field

S – entropy

θ - temperature

i – 1, 2, 3, 4, 5, 6

m – 1, 2, 3

Then it follows,

$$\frac{\partial D_m}{\partial T_j} = \frac{\partial S_j}{\partial E_m} = d_{mj}^{H,\theta} \qquad \text{Piezoelectric constant}$$

$$\frac{\partial B_m}{\partial T_j} = \frac{\partial S_j}{\partial H_m} = d_{mj}^{E,\theta} \qquad \text{Piezomagnetic constant}$$

$$\frac{\partial D_m}{\partial \theta} = \frac{\partial S}{\partial E_m} = p_m^{T,H} \qquad \text{Pyroelectric constant}$$

$$\frac{\partial B_m}{\partial \theta} = \frac{\partial S}{\partial H_m} = i_m^{T,E} \qquad \text{Pyromagnetic constant}$$

$$\frac{\partial D_m}{\partial H_k} = \frac{\partial B_k}{\partial E_m} = m_{mk}^{T,\theta} \qquad \text{Magneto-dielectric constant} \qquad \text{(C.10)}$$

$$\frac{\partial S_j}{\partial \theta} = \frac{\partial S}{\partial T_j} = \alpha_j^{E,H} \qquad \text{Thermal expansion constant}$$

$$\left(\frac{\partial S_i}{\partial T_j}\right)_{E,H,\theta} = s_{ij}^{E,H,\theta} \qquad \text{Elastic compliance}$$

$$\left(\frac{\partial D_m}{\partial E_k}\right)_{T,H,\theta} = \epsilon_{mk}^{T,H,\theta} \qquad \text{Dielectric constant}$$

$$\left(\frac{\partial B_m}{\partial H_k}\right)_{T,E,\theta} = \mu_{mk}^{T,E,\theta} \qquad \text{Permeability constant}$$

Here,

j – 1, 2, 3, 4, 5, 6

m – 1, 2, 3

Pyroelectricity is the generation of a temporary voltage in a certain material when subjected to a temperature change. The temperature change makes the atoms move slightly changing the polarization of the material. This polarization causes a generation of voltage. Similarly pyromagnetism is the generation of a magnetic field due to a temperature change.

In a piezoelectric medium stress is a function of not only the geometric strain but also of the electric field. In practice effects of magnetic fields are ignored when dealing with piezoelectric materials and effects of electric fields are neglected when considering magnetic

materials. For piezoelectric materials that are not pyroelectric, piezoelectric and dielectric constants are similar whether it's in adiabatic or isothermal conditions.

Piezoelectric media are anisotropic. For any direction of propagation there are three possible acoustic waves with mutually perpendicular directions of vibration and in general with different velocities. General wave equation can be written as,

$$\rho \frac{\partial^2 \xi_1}{\partial t^2} = c_{ik}^E \frac{\partial^2 \xi_k}{\partial x^2} - e_{ki} \frac{\partial E_k}{\partial x} \quad \text{(C.11)}$$

Where

ρ - density of medium

c – elastic constant

Acoustic waves in piezoelectric semiconductors can be amplified or attenuated by applying a dc electric field parallel to the propagation direction. The interaction of the direct current in the piezoelectric medium with the elastic wave creates a travelling ac electric field. Coupling between electromagnetic waves due to piezoelectric effect is negligible. Mechanical damping gives rise to an additional force on a unit volume which is proportional to the velocity of the wave.

C.4 Piezoelectric properties of materials

Piezoelectric constants are proportional to the electric field generated by a unit mechanical stress or alternatively to the mechanical strain produced by a unit electric field.

Table C.1: Piezoelectric constants of $LiNbO_3$, $LiTaO_3$ and PZT [7]

Piezoelectric Constant	Lithium Niobate	Lithium Tantalate	PZT-4 (Navy Type I)
d_{15} ($x10^{-11}$ C/N)	6.8	2.6	50.0
d_{22}	2.1	0.7	
d_{31}	-0.1	-0.2	-12.2
d_{33}	0.6	0.8	29.5
e_{15} (C/m^2)	3.7	2.6	
e_{22}	2.5	1.6	
e_{31}	0.2	0.0	
e_{33}	1.3	1.9	
g_{15} ($x10^{-2}$ m^2/C)	9.1	5.8	3.9
g_{22}	2.8	1.5	
g_{31}	-0.4	-0.6	-1.06
g_{33}	2.3	2.1	2.49
h_{15} ($x10^9$ N/C)	9.5	7.2	
h_{22}	6.4	4.3	
h_{31}	0.8	0.0	
h_{33}	5.1	5.0	

C.4.1 PZT Ceramic

PZT is the inorganic compound lead zirconate titanate with the chemical formula $Pb[Zr_xTi_{1-x}]O_3$ ($0 \leq x \leq 1$). It is renowned for its piezoelectric effect which has many applications. When compressed there occurs a potential difference across two of its faces. When an external electric field is applied a change in its physical shape occurs. It is also pyroelectric and ferroelectric adding to its applications. PZT is used in producing ultrasound transducers, sensors, actuators, ceramic capacitors as well as ceramic resonators for reference timing in electronics circuitry. It is commercially used not in its pure form but rather doped with acceptors or donors. Acceptors create oxygen vacancies and donors create metal vacancies to facilitate domain wall motion. Acceptor and donor doping create hard and soft PZT respectively differing in piezoelectric constants. Soft PZT has a higher piezoelectric constant and higher losses whereas hard PZT has a lower piezoelectric constant and lower losses. One of the more commonly used PZT ceramics is $PbZr_{0.52}Ti_{0.48}O_3$. It has a higher piezoelectric response and poling efficiency due to the increased number of allowable domain states. PZT is a metallic oxide based piezoelectric material found in the Tokyo institute of technology around 1952. It is formed under extremely high temperatures. Compared to the previously discovered piezoelectric material barium titanate, PZT has a higher sensitivity and a higher operating temperature. Other material characteristics include high dielectric constant, high coupling, high charge sensitivity, high density with a fine grain structure, high Curie point and a noise free frequency response.

C.5 Applications

C.5.1 Interdigital transducers

The advantage of surface acoustic waves (SAW) is that they are accessible at the surface making them be adapted to the technology easily. The acoustic energy is usually contained within 1 to 100μm from the surface. Thus it's easy to construct a delay line travelling along the surface. Because of the easy accessibility of the surface, a delay line can be tapped at several points creating a transversal filter.

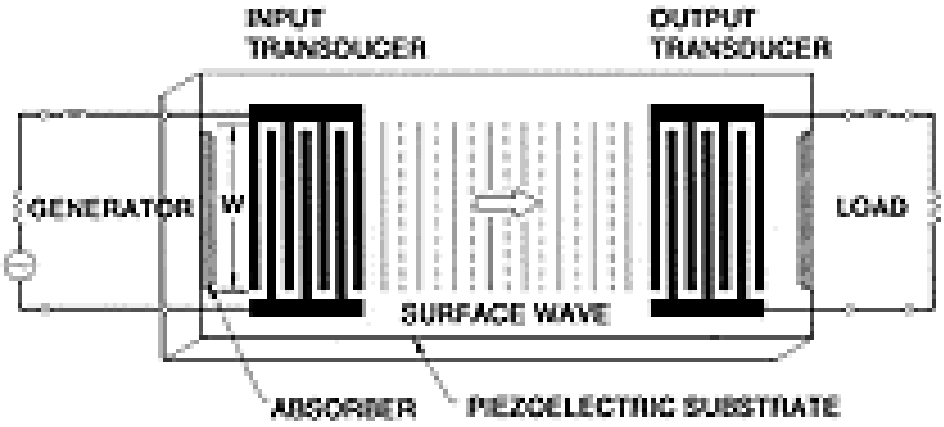

Fig. C.2: Excitation and detection of surface acoustic waves by an interdigital transducer

Interdigital transducers convert an electric signal into a surface acoustic wave and reconvert it into an electric signal. These are usually used to excite surface acoustic waves in a piezoelectric material. As shown in figure C.2, an electric field excites a surface acoustic wave in the piezoelectric substrate and it is reconverted to an electrical signal at the electrode at the other

end. It is efficient to use an interdigital transducer consisting of several pairs of electrodes or fingers. A pair of electrodes excites a Rayleigh wave and these combine to form a large enough acoustic signal. Frequency is chosen such that between each two fingers there is one wavelength. A transducer with many fingers works efficiently over a narrow frequency range and is used to filter various frequency signals from one another.

C.5.2 Network theory of the transducer

The network theory is an equivalent circuit method on the idea that the response of a single finger is similar to that of a bulk wave transducer. It is useful in determining the electrical input impedance and the frequency response of an interdigital transducer. Another approach is the use of the normal mode formalism which is based on the conservation of power. Another is based on wave impedance concepts. Yet another one is a direct solution of the field theory.

Electrical equivalents to the acoustic force F_i and terminal velocity V_i are defined as [3],

$$V_i = \frac{F_i}{\phi} \tag{C.12}$$

Where ϕ is the transformer ratio,

$$\phi = \frac{hC_s}{2}$$

h – piezo constant

C_s – capacitance of one periodic section

Then the mechanical impedance Z_0 of the substrate can be expressed as,

$$\frac{Z_0}{\phi^2} = \frac{2\pi}{\omega_0 C_s K^2} \quad \text{(C.13)}$$

Where,

$\omega_0 = 2\pi v/l$ = synchronous frequency

v – acoustic velocity

l – periodic length of the system

K – effective electromechanical coupling constant

Electromechanical coupling constant is the change of velocity of the wave in the medium when the RF field between the electrodes is shorted out. Using the ratio of stiffened and unstiffened velocity of a piezoelectric medium ($\Delta V/V$), the fractional change in velocity of a bulk wave transducer when there is no electric field within the medium can be obtained as,

$$\frac{\Delta V}{V} = \frac{-K^2}{2} \quad \text{(C.14)}$$

A correction factor is added to compensate for the effect of changing the finger width and (C.14) can be written more generally as,

$$K^2 = 2f \left|\frac{\Delta V}{V}\right| \quad \text{(C.15)}$$

Where,

f – filling factor

C.5.3 Bulk acoustic wave transducers

The transducer element is a cut from an oriented piezoelectric crystal. This makes the transverse and longitudinal waves emitted perpendicular to the faces. Electrodes which are generally vacuum deposited gold on a thin chromium film, are at the opposite faces as shown in figure C.3(a) The electrodes ate usually about 0.5μm in thickness.

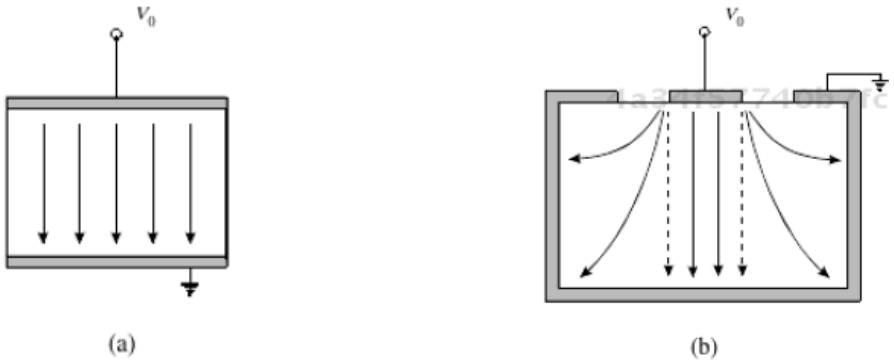

Fig. C.3: Electric field in an (a) ideal thickness mode piezoelectric transducer and (b) One with coaxial electrode configuration [1]

VITA

SAMINDA ADIKARAM

401, Hathorn rd., Apt. I-202A, Oxford, MS 38655 • (662) 801-7454 • ssadikar@go.olemiss.edu

EDUCATION

BSc., Physical Sciences, University of Peradeniya, Sri Lanka, June 2009

TEACHING EXPERIENCE

Laboratory Instructor, 2010 – present
University of Mississippi
Course: Astronomy

Research Assistant, 2011
National Center for Physical Acoustics
High intensity focused ultrasound

Grader, 2011 & 2012
University of Mississippi
Course: General Physics

Grader, 2012
University of Mississippi
Course: Physics for Science and Engineering

Laboratory Instructor, 2012
University of Mississippi
Course: Laboratory Physics

Research Assistant, 2013
University of Mississippi
Group Velocity of Acoustic Waves in Plates of Electronic Materials

HONORS AND FELLOWSHIPS

Zdravko Stipcevic Honors Fellowship, 2010 – 2011
Member, Mississippi Academy of Sciences, 2014 – present

PUBLICATIONS AND PRESENTATIONS

Saminda Adikaram, Igor Ostrovskii, Chandrima Chatterjee (2014), Lamb Wave Propagation in Electronic Material Plates, Mississippi Academy of Sciences (MAS) 78th annual meeting